EARTH SURFACE PROCESSES AND LANDFORMS
Earth Surf. Process. Landforms **36**, 1023–1043 (2011)

Published online 18 February 2011 in Wiley Online Library
(wileyonlinelibrary.com) DOI: 10.1002/esp.2129

Sediment dynamics below retreating cliffs

D. J. Ward,[1,2]* M. M. Berlin[3] and R. S. Anderson[1,2]
[1] Institute of Arctic and Alpine Research, University of Colorado, Boulder, CO, USA
[2] Department of Geological Sciences, University of Colorado, Boulder, CO, USA
[3] Community Surface Dynamics Modeling System, University of Colorado, Boulder, CO, USA

Received 14 August 2009; Revised 28 November 2010; Accepted 7 December 2010

*Correspondence to: D. J. Ward, Department of Earth and Planetary Sciences, University of New Mexico, Albuquerque, NM, USA. E-mail: djward@unm.edu.

ESPL
Earth Surface Processes and Landforms

ABSTRACT: The retreat of cliffs may constitute the dominant erosional response to base-level fall in arid settings underlain by horizontally-bedded sedimentary rock. These vertical cliffs typically loom above a relatively straight bedrock slope ('plinth') that is mantled with a thin layer of sediment and perched near the angle of repose. In detail, a plinth consists of a system of quasi-parallel ridges and channels. We ask how the sediment supplied from a retreating cliff influences the erosion of the plinth hillslopes and channels, and how this affects the rate of cliff retreat. Motivated by field observations and high-resolution topographic data from two sites in western Colorado, we develop a two-dimensional (2D), rules-based numerical model to simulate the erosion of channels draining a plinth and diffusive erosion of the intervening interfluves. In this model, retreat of a cliffband occurs when the height of the vertical cliff exceeds a threshold due to incision by channels on the plinth below. Debris derived from cliff retreat is distributed over the model plinth according to the local topography and distance from the source. This debris then weathers in place, and importantly can act to reduce local bedrock erosion rates, protecting both the plinth and ultimately the cliff from erosion. In this paper, we focus on two sets of numerical model experiments. In one suite, we regulate the rate of rockfall to limit the cliff retreat rate; in most cases, this results in complete loss of the plinth by erosion. In a second suite, we do not impose a limit on the cliff retreat rate, but instead vary the weathering rate of the rockfall debris. These runs result in temporally steady cliff-plinth forms and retreat rates; both depend on the weathering rate of the debris. Copyright © 2011 John Wiley & Sons, Ltd.

KEYWORDS: hillslope; cliff retreat; escarpment; numerical model

Introduction

Throughout the Colorado Plateau and in other settings with horizontally-bedded rocks of varying erodibility, vertical cliffs often sit above a straight slope at or near the angle of repose, which here we call a plinth (Figure 1). In some instances the cliff appears to have retreated in response to base-level fall associated with recent incision of a local trunk stream (e.g. the Colorado River). In other instances, cliffs appear to have retreated without direct base-level influence. However, the prevalence of this morphology bears explanation. In particular, we are interested in how plinth lowering may influence the rate of cliff retreat, which in turn may affect sediment dynamics on the plinth by supplying coarse debris. We discuss this mechanism as a feedback by which the input of coarse debris into the small channels and onto the hillslopes within the plinth regulates the rate of cliff retreat.

Although the mechanisms of cliff retreat have received much focus (e.g. Oberlander, 1977; Howard, 1988, 1995; Howard and Selby, 1994; Luo *et al.*, 1997; Weissel and Seidl, 1997; Lamb and Dietrich, 2009) few of these studies have quantitatively addressed the plinth system and its response to rockfall debris. King (1953) described escarpment slopes in terms of four elements, moving down in elevation: the waxing slope, the free face (cliff), the detrital slope (plinth) and the waning slope. If the free face and detrital slope are actively eroded, the hillside will retreat parallel to itself. Koons (1955) outlined the basic model of retreat of an escarpment in soft rocks with a hard caprock (Figure 2). According to his conceptual model, after initiation of the escarpment by fluvial incision or faulting, slopes adjust to angles concomitant with the bulk strengths of the rocks in which they are formed. A vertical cliff forms in competent caprock above a soft rock plinth of 34° to 38°. This plinth is eroded by small channels, rills, sheetwash, and diffusive mechanisms, propagating the vertical cliff downward into the soft rock unit. Once this cliff is too high to be supported by the unbuttressed soft rock, it collapses to an angle of 40° to 50°, forming a talus slope at ~32° on the plinth. To continue retreat of the cliff, this talus must eventually be removed, leaving a new bare rock plinth at 34°–38°.

We modify this basic conceptual model to account for regolith transport, both in the first-order channels that drain the plinth and down the ridges that separate them. Here, 'regolith' signifies mobile material on the Earth's surface, derived from weathering of bedrock or rockfall debris. Regolith includes soil and bedload in streams. 'Debris' is used to refer to the products of rockfall, whether they are mobile or not. Crosswise relief developed on most plinths suggests that regolith travels in a direction that is oblique, rather than perpendicular, to the trend of the cliff. We argue that it is this crosswise motion from cliff-perpendicular ridges to cliff-perpendicular channels that

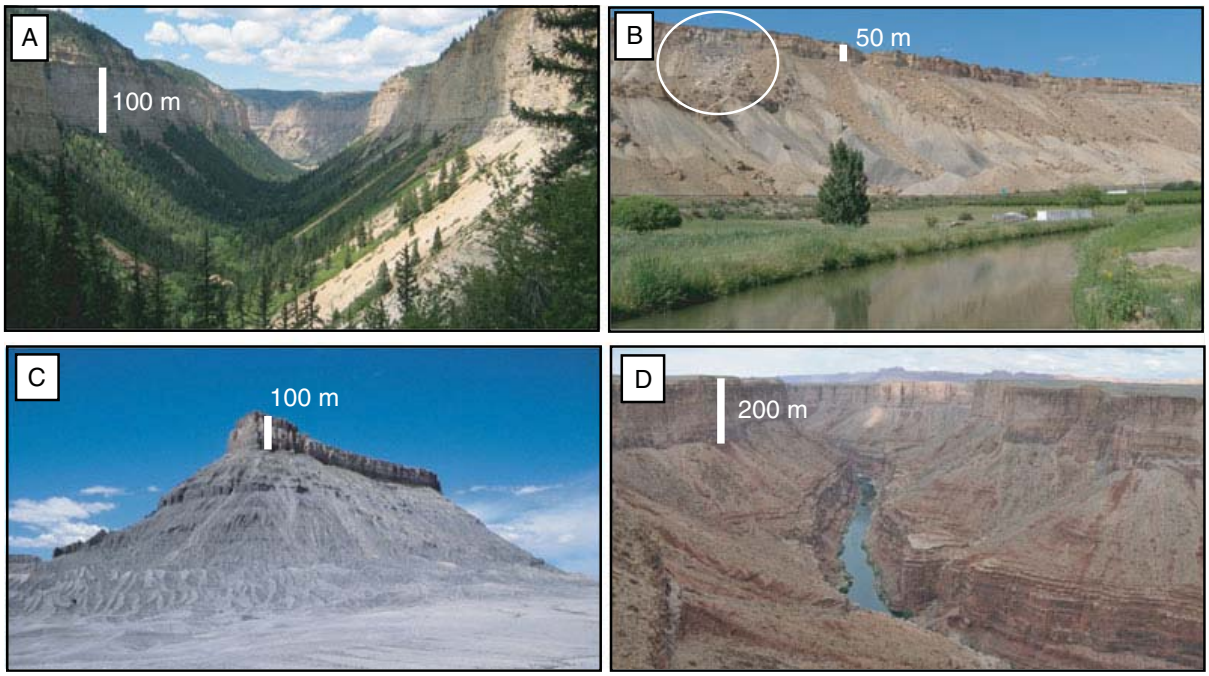

Figure 1. Photographs of cliffs on the Colorado Plateau and approximate cliff heights. (A) East Fork Parachute Canyon on the Roan Plateau, Garfield County, Colorado; view is looking downstream. (B) Book Cliffs west of Mt Garfield, Mesa County, Colorado (July 9, 2009 rockfall debris is circled), agricultural ditch in foreground; Colorado River is approximately 3·5 km from the cliff. (C) Factory Butte, Wayne County, Utah. (D) Marble Canyon, Colorado River, Coconino County, Arizona. This figure is available in colour online at wileyonlinelibrary.com/journal/espl

allows a nearly straight plinth profile. The magnitude of topographic relief within the plinth is related to the amount of regolith produced by weathering of the plinth bedrock, the transport capacity of the plinth channels, and the stochastic delivery of rockfall debris from the cliff above. As case studies of this conceptual model, we document the detailed morphology of plinth hillslopes from two sites in western Colorado using digital elevation model (DEM) data derived from Airborne Laser Swath Mapping (ALSM).

The interaction between the delivery of rockfall debris and the transport processes that must carry it off the plinth represents a potentially strong feedback on the overall rate of retreat. In this paper, we explore the dynamic role of rockfall debris in affecting the morphology of the plinth through both its coverage of plinth rocks and its ability to rearrange the drainage network on the plinth. To experiment with the ways in which these different behaviors and materials interact requires the use of a two-dimensional (2D) simulation. We use the DEM measurements and field observations to develop a numerical model that codifies certain elements of our conceptual model. Model results demonstrate that the quantity and durability of debris supplied from cliff retreat can strongly affect both the morphology of the escarpment and the rate of its retreat.

Field Areas

We target two example landscapes of the morphology that can result from the processes of plinth lowering and cliff retreat: the Book Cliffs and canyons within the Roan Plateau in western Colorado (Figure 3). We use these two sites because they share a similar morphology (Figure 1) characterized by a vertical cliff above a straight bedrock slope, yet are eroded into different bedrock and appear to have different base-level controls. We use ALSM data collected through National Center for Airborne Laser Mapping (NCALM) seed grants to identify key morphologic properties (see section later entitled 'Topographic Data from LiDAR DEM'), which we can then use to develop conceptual and numerical models.

Book Cliffs

The Book Cliffs are a dominantly east–west striking escarpment in western Colorado and Utah (Figure 3). The cliffs span over 200 km in geographic distance and have an average topographic relief of ~1000 m. Near Palisade, at the far eastern end of the Book Cliffs, Upper Cretaceous Mesaverde Group Sandstone caps the cliffs in several layers, each several tens of meters thick. Beneath this is the Mancos Shale, hundreds of meters of it, that underlie the valley through which the Colorado River flows. The stratigraphy is part of a broad monocline related to the Uncompahgre Upwarp, a Laramide monocline of the Colorado Plateau. The layers dip northeast at approximately 5° near the town of Palisade, and are backtilted with respect to the face of the cliffs. We target the more simple morphology at the south-eastern end of the Book Cliffs near Mt Garfield (Figure 3). Farther northwest, the cliff becomes more deeply indented; this is likely a result of the dipping stratigraphy. To the north along the escarpment, the north-dipping, resistant sandstone units outcrop lower and lower in the cliffband. These units act as local base level for streams draining the escarpment, and because the base level lowers in time due to the structural dip, the drainages pinned to it expand. This is similar to the steepening of stream profiles on the upper Roan Plateau surface due to the dip of the Mahogany layer (Berlin and Anderson, 2009; see also later).

On the simpler plinth to the southeast, vertical cliff heights are generally around 50 m, and the straight slope (plinth) beneath the cliff is typically 500 m in horizontal length before it flattens and grades into the valley floor (Figure 1). Over long time scales, the base level for the Book Cliffs is controlled by the Colorado River to the south, which flows roughly east–west (at a distance of 5 km to over 20 km from the ALSM swath). The

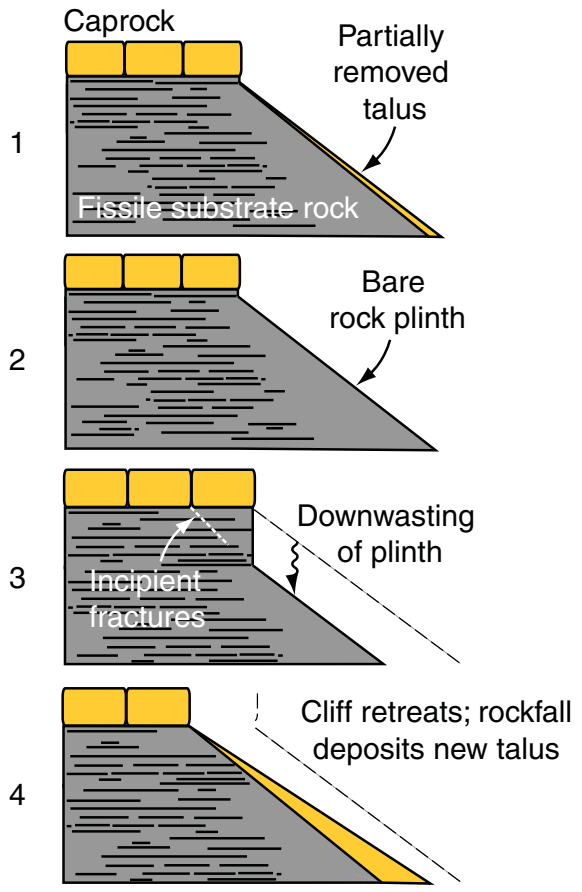

Figure 2. Stages of cliff retreat after Koons (1955). (1) Profile of an escarpment with a thin mantle of talus from previous rockfalls. (2) As this talus is removed from the plinth, a bare rock slope develops with an angle of ~38°. (3) Erosion of the bare plinth proceeds, propagating the break in slope downward until the vertical height of the cliff cannot be supported by the strength of the rock. At this point, rockfall occurs and a new talus cover develops at an angle of repose slope of ~32° armoring the plinth and shutting down further retreat until the talus is removed (4). This figure is available in colour online at wileyonlinelibrary.com/journal/espl

straight shale plinth is heavily channelized, although on average the slope angle of the surface perpendicular to the trend of the cliff is ~34°. The upper several hundred meters of the plinth is strewn with debris from the sandstone cliffs above; this debris ranges in size from silt to ~10-m diameter boulders. To some extent, this accumulation of debris may be a relict of increased rockfall due to climatic conditions at some time in the past (e.g. Schmidt, 2009). However, the escarpment is clearly an active rockfall source in modern times.

The July 9, 2009 Palisade rockfall

At 5:44 a.m. on July 9, 2009, a Mw 2.5 earthquake was recorded near Palisade, Colorado. A concomitant rockfall on the Book Cliffs was witnessed by many due to its visibility from I-70 and drew the attention of media outlets as far away as Denver. Further examination of the seismic data by the National Earthquake Information Center at the US Geological Survey supports the interpretation that the earthquake was in fact the vibration from the rockfall.

Field investigation within three days of the rockfall event revealed that a 120-m wide by 50 m high by several meters thick slab had toppled forward from the cliff, landing face-first on the slope below the cliff (Figure 1). Most of the debris was contained in a single runout, which was nearly planar but was slightly concave-up in longitudinal profile. This runout was 270 m in horizontal length and rested at an average slope angle of 34°. The downslope length was therefore 380 m. Within this area, debris seemed to be evenly spread and randomly oriented; it was difficult to estimate its thickness as it lay on a slope covered with older debris. Nonetheless, the average thickness was probably not more than a few meters. Debris sizes ranged from silt to 15-m diameter boulders, and were distributed similarly to the older debris on the same slope. Darker boulders of the shale underlying the sandstone caprock were found in the top quarter or so of the runout distance, corroborating a face-first toppling mode of failure. Outlying boulders were scattered sparsely within tens of meters of the edges and for many hundreds of meters downslope of the main runout.

The east end of the runout was bounded by a 2–4 m wide and 1–2 m deep gully that channeled the tumbling debris; fresh erosion of the shale bedrock in this gully appeared to have been caused by dry rock debris flowing through it. We observed a similar but smaller channel in the west edge of the runout nearer the base of the cliff. Divots of half-meter size and several centimeters deep were common on exposed shale bedrock within and near the runout area, where boulders had bounced in transit. Some of the boulders apparently broke up on impact or later. One boulder had a fracture across it and fell apart with only light prompting from a walking stick. We observed fresh fracture faces on older boulders that had been on the slope previously and had been hit and broken by falling rocks from the recent event. Loose fines were piled up tens of centimeters deep on the uphill sides of several of the biggest boulders in the slide, suggesting that the boulders came to rest while smaller debris was still in motion in the runout area.

At the location of the rockfall, the base of the sandstone caprock is about 300 vertical meters above the river valley. The base of the vertical cliffband is commonly etched into the shale by 1 to 5 m below the base of the sandstone. This shale portion of the cliff is highest where the channel heads of the plinth drainage reach the base of the cliffs, suggesting that channel erosion can efficiently expose and perhaps undermine portions of the cliff. The Book Cliffs are therefore a useful example for studying the dual processes of cliff retreat and plinth evolution, due to the contrast in erodibility between the resistant sandstone caprock and the weaker shale plinth. This contrast means that debris derived from cliff retreat may exert an important influence on plinth evolution by shielding the underlying shale from erosion.

Roan Plateau

The Roan Plateau in western Colorado is drained on its southern edge by tributaries to the upper Colorado River. Each stream that drains the plateau contains a single large knickpoint (~100-m waterfall), which is presumably related to late Cenozoic incision of the upper Colorado River. The plateau bedrock consists of laterally continuous Eocene lake sediments, including the Green River Formation, and knickpoint elevations are correlated with the outcrop of a resistant oil-shale layer, called the Mahogany ledge (Hail, 1992). A stream power-based celerity model (e.g. Crosby and Whipple, 2006) works well to predict the positions of knickpoints on Roan Plateau streams, such that knickpoint retreat rate is a power function of drainage area and is proportional to rock susceptibility to erosion (Berlin and Anderson, 2007). Knickpoint initiation into the Roan Plateau at ~8 Ma is constrained by Colorado River incision rate data and a reconstructed elevation of the Mahogany oil-shale zone at the Colorado

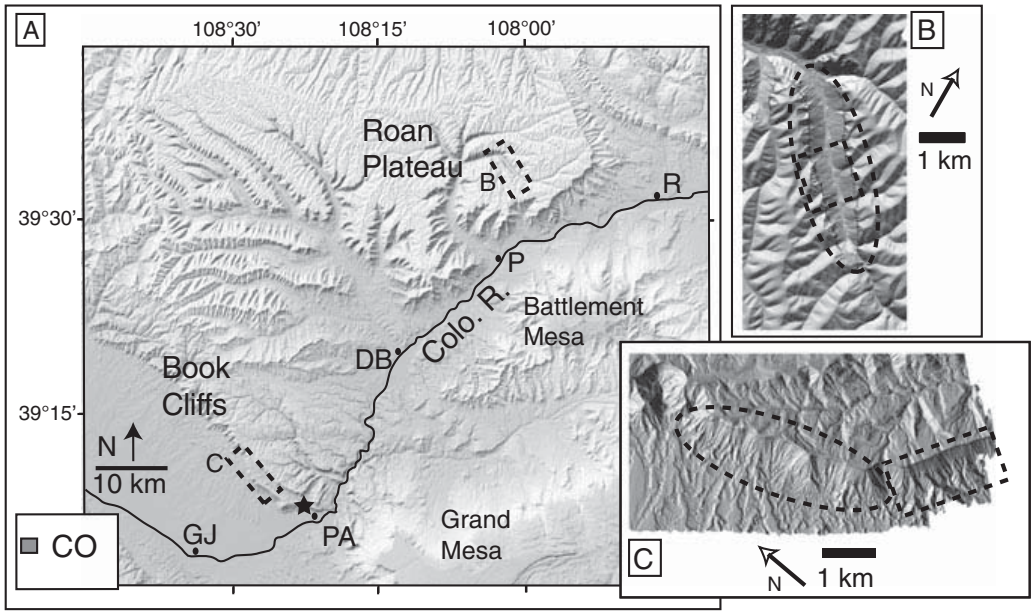

Figure 3. (A) Shaded relief of portion of western Colorado. Colorado River flows from east to west. Dashed boxes indicate ALSM data for Book Cliffs and Roan Plateau. DB: DeBeque, GJ: Grand Junction, P: Parachute, PA: Palisade, R: Rifle. Star near Palisade indicates location of July 9, 2009 rockfall discussed in text. (B, C) Shaded relief images of ALSM-derived DEM for Roan Plateau and Book Cliffs, respectively. Dashed rectangles indicate approximate locations of profiles shown in Figures 7 and 8. Dashed ovals indicate other profile locations used to collect statistics on hillslope morphology plotted in Figure 9.

River confluence (Berlin and Anderson, 2007). Models of the many streams draining the Roan Plateau suggest rapid initial knickpoint propagation rates, which decline as drainage area decreases step-wise at tributary junctions to modern rates of a few millimeters per year (Berlin and Anderson, 2007). Upstream of the prominent knickpoints, the downstream portions of streams have steepened slightly due to structural and lithologic controls on knickpoint elevation (Berlin and Anderson, 2009).

Downstream of each knickpoint is a steep-walled canyon (Figure 1A) that is cut largely into the Parachute Creek Member of the Green River Formation, which consists of fine-grained sandstones and lacustrine shales, including oil shale. Cliff heights on each canyon wall are generally around 100 m, and the straight slope beneath the cliff is typically 100–400 m in horizontal length before it abruptly levels off into the valley floodplain. Channels flowing down the plinth that lack drainage area above the cliff band are remarkably straight, with a slope angle of 34°. Channelization is less pronounced than on the Book Cliffs, resulting in lower interfluve relief. Sediment cover on the plinth surface is variable and thin. Near the canyon heads, the underlying bedrock stratigraphy is clearly visible through the thin and discontinuous regolith cover. Farther downstream, sediment may cover the plinth to an unknown depth. Field observations in a few locations have revealed multiple generations of fine-grained (gravel-sized) rockfall debris that has not yet been evacuated from the system (Berlin, 2009).

We assume that canyon widths on the Roan Plateau may record progressive hillslope response to channel incision associated with upstream migration of the knickpoint. The canyons widen with distance downstream from each knickpoint. Canyon width increases most at the canyon head and more gradually farther downstream, such that canyon width and canyon relief tend to increase at a similar rate with distance downstream from each knickpoint (Berlin, 2009). This pattern implies a strong coupling between the processes of channel incision, hillslope lowering, and canyon wall retreat. In order for canyon widening to keep pace with channel incision, the canyon side slopes must very efficiently lower in elevation as well as transport material derived from cliff retreat. Relating modern canyon widths to the Berlin and Anderson (2007) knickpoint retreat model allows one to predict cliff retreat rates of 0·25 to 1 mm/yr (Berlin, 2009); these rates have not been verified with field measurements. Roan Plateau canyons contain evidence of prior large landslide events (e.g. Olson, 1974); however, debris grain sizes on the plinth make it difficult to distinguish between the rapid collection of larger blocks in transit downslope and the failure of individual small blocks.

Rocks on the Roan Plateau exhibit more subtle contrasts in erodibility when compared with the Book Cliffs. Here, material derived from cliff retreat may not be dramatically different from the plinth bedrock, such that it may not provide a shielding effect. However, if the rate of cliff retreat is indeed limited by the lowering rate of the plinth (Berlin, 2009), then material derived from cliff retreat must be eroded before subsequent cliff retreat can occur.

Modern climate and vegetation

Average annual precipitation at lower elevations in the Book Cliffs and Roan Plateau area generally increases to the east, from ~22 cm in Grand Junction to ~29 cm in Rifle (Western Regional Climate Center Station 057031, http://www.wrcc.dri.edu/, accessed January 2010). At higher elevations, average annual precipitation can reach up to 50–65 cm (Taylor, 1987; BLM, 2004). Between October and April, most of the precipitation falls as snow, whereas thunderstorms provide precipitation during the summer months. Peak stream discharges are associated with snowmelt runoff and occur between late April and late May. Records from 13 US Geological Survey gages on streams that drain the Roan Plateau (periods of record between 6 and 25 years) indicate that mean annual discharge ranges from 0·02 to 1·25 m^3/s. Maximum daily flows of up to 60 m^3/s have

been measured at Roan Plateau gages with larger drainage areas. Groundwater flow from seeps and springs does contribute to surface runoff, although discharge measurements between 1981 and 1983 from springs on the Roan Plateau indicate a mean annual discharge of only $\sim 3 \times 10^{-4}$ m^3/s (based on measurements at 129 springs) (Butler, 1985). The small, ephemeral channels that drain the Book Cliffs have not been gauged. Vegetation types and abundance are sensitive to elevation, gradient, and aspect, with mature aspen and conifer forests on the higher elevation of the Roan Plateau, and pinyon, juniper and sagebrush being more prevalent in the Book Cliffs area.

Conceptual Model

We generalize the landscapes discussed earlier (e.g. Figure 1) to the conceptual model depicted in Figure 4. We divide the escarpment into two systems: the cliff system, which extends from the top of the caprock down to the base of the vertical cliff at the top of the plinth, and the plinth system, which includes the hillslopes and channels from the base of the cliff down to local base level. The cliff system sets the debris supply, and affects the water supply and water energy for the plinth system. The plinth system sets the rate of downwearing at the cliff base in the cliff system. The physical processes important to each of these systems differ; in this contribution, we assume that the local height of the vertical cliff is the important criterion for failure of the cliff, and focus on the processes of plinth erosion that set this height. In order for cliffs to maintain constant form as they retreat, a combination of these processes must undermine or otherwise remove cliff material, transport debris away from the base of the cliff, and erode the plinth surface. If debris is not transported away from the cliff, then the cliff may eventually be 'consumed' by the talus-mantled plinth (Selby, 1982).

The overall morphology of the escarpment is therefore set by the ratio of plinth downwearing to cliff backwasting. Initially, divergence of regolith flux at the rocktype boundary leads to downwearing of the plinth-cliff contact. The plinth lowers until the regolith flux transported away from the plinth top equals the regolith flux coming in from the cliff (in the form of rockfall debris). If this never occurs, the plinth wears completely away, leaving a purely vertical cliff. Both hillslope and channel processes on the plinth may act to set the outgoing regolith flux. Any combination of cliff and hillslope processes may determine the incoming flux, which may increase with the height of the cliff (Table I).

Plinth process competition

The morphology of both the Book Cliffs and Roan Plateau escarpments (as well as many others) suggests that several erosion and transport processes on the plinth conspire to accommodate the required flux of regolith (Figure 4). Channels that drain the plinth generally run perpendicular to the trend of

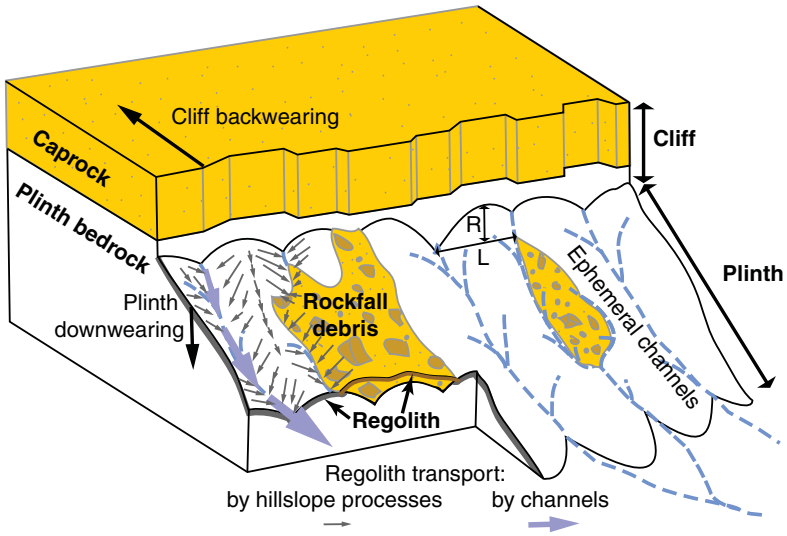

Figure 4. Conceptual model relating rockfall from the backwearing cliff, regolith production and transport on the plinth, and downwearing of the plinth. Rockfall debris fills in and diverts channels. Interfluve relief (R) is set by the channel spacing (L) and the weathering rate of plinth bedrock, except where disrupted by rockfall. Regolith, produced by weathering of both bedrock and debris on the plinth, moves down local fall lines into channels, where it can be removed efficiently by occasional flows of water. The downwearing rate of any location on the plinth surface is proportional to the local divergence of regolith flux. This figure is available in colour online at wileyonlinelibrary.com/journal/espl

Table I. Examples of factors influencing regolith flux onto and off of the plinth

Factors that increase the flux off the plinth	Factors that decrease the flux off the plinth	Factors that increase the flux onto the plinth
• Steeper channels • Faster sediment transport in streams • Bigger catchments • Faster regolith transport on hillslopes • Higher relief – more efficient transfer from hillslopes to channels	• Slower-weathering rock or rock debris • Larger grain sizes, slower sediment transport • Lower-angle plinth (channels)	• Taller cliff to shed rock • Faster-eroding cliff • Sediment delivery from above the cliff • Faster-eroding plinth (rock to regolith) • Higher relief – more surface area for regolith production

the cliff; these channels focus the delivery of water and sediment downslope, thus eroding the plinth. Divides between these channels, also perpendicular to the cliff, erode by hillslope processes such as creep, sheetwash, and rainsplash, in a diffusion-like manner. This material is transported both down the plinth and across it, away from the divides and into the channels. The competition between the advective channels and the diffusive hillslopes sets the relief and drainage spacing on the plinth (e.g. Perron *et al.*, 2008).

This competition between processes explains why plinth profiles are commonly straight, rather than convex. In general, unchanneled hillslopes are convex because the amount of regolith that must be transported increases downslope due to additions by weathering of bedrock. Transport of this added material is accommodated by a downslope increase in slope. However, on a plinth (which could be viewed as a long, planar hillside), parallel channels carry some fraction of the regolith. Transport vectors from the hillslopes into these channels are oblique to the cliffline and short relative to the length of the plinth. Because the carrying capacity of the channels increases downstream with drainage area, and the hillslopes can offload their regolith laterally into the channels, the overall slope of the plinth does not need to increase toward its base; it is controlled mainly by the slope of the channels.

By this model, faster regolith production from plinth bedrock leads to more crosswise plinth relief and higher crosswise curvatures, while down-plinth hillslope profiles (i.e. the crests of parallel ridges) remain straight because they always have a similar, small amount of regolith to transport. For instance, in a steady case where regolith transport rate increases linearly with slope, 'steady-state' ridge-to-valley relief (R) is directly proportional to the regolith production rate $\dot{w}$:

$$R = \frac{\dot{w}}{2k} L^2, \tag{1}$$

where k is a transport coefficient and L is the spacing between channels downcutting at a steady rate (e.g. Culling, 1960). Transport relations that are non-linear with slope (e.g. Roering *et al.*, 2001) lead to uniform 'threshold" slopes, faster response to external forcing, and lower channel to hilltop relief.

The influence of rockfall debris

Cliff retreat typically proceeds spasmodically in time (e.g. Oberlander, 1977). Periods of limited rockfall activity are punctuated by occasional large rockfall events that instantaneously introduce large amounts of debris onto the plinth. Blockfall and landslides from the cliff contribute debris to the entire plinth surface, although material will preferentially accumulate in the channels. The area of the plinth that is debris-covered depends on the rate of supply and the rate at which immobile debris breaks down into transportable regolith or sediment. In some settings, the debris size and quantity may be within the transport capacity of the extant drainage network. In this case, the channel network should be little impacted by the debris. If, however, the rockfall debris is not transportable by the existing channels, and weathers slowly, the channels must adjust to incise through or around this material; the channels effectively become detachment-limited. In the Book Cliffs and similar areas where the plinth bedrock is more erodible than the overlying rockfall debris, this incision occurs by the propagation of meter-scale knickpoints within and alongside the debris field (Figure 5). The dominant channels are found at the edges of debris fields, preferentially on the weaker bedrock. Ultimately, channels may abandon the debris field as a ridge, thus inverting the topography.

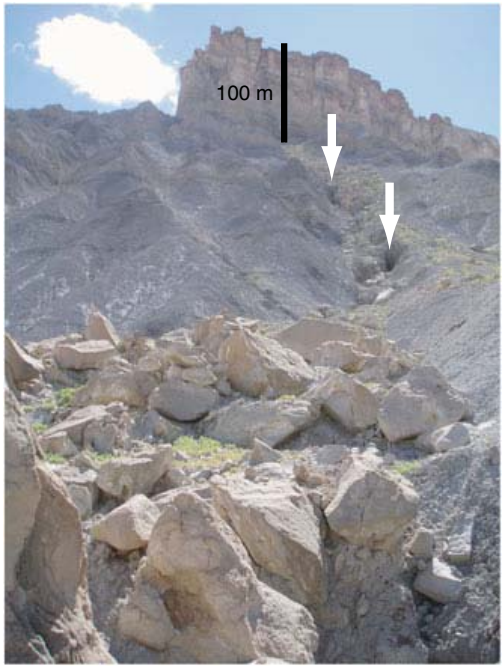

Figure 5. A debris-filled channel on Factory Butte (Figure 1C). Photographer was standing at the base of a small knickpoint like the two highlighted with arrows. Here (as in the stratigraphically similar Book Cliffs), the debris is harder to erode than the bedrock. This leads new channels to form alongside the debris field through knickpoint propagation, eventually inverting the topography. Meanwhile, the debris weathers to more mobile material and is additionally redistributed down slopes, ultimately dispersing it and diminishing its effect on shielding the bedrock, unless fresh rockfall replenishes it. This figure is available in colour online at wileyonlinelibrary.com/journal/espl

Hillslopes within the plinth drainage system can also become covered in debris, particularly those with low relief and slope angles. As in the case of the channels, coverage by resistant, immobile debris effectively results in a conversion to detachment-limited conditions. The limiting process becomes breakdown of the debris into regolith that is transportable by hillslope processes such as rainsplash, wind, and surface wash. Furthermore, channelization of these hillslopes is also suppressed by the presence of resistant caprock debris. The presence of debris can therefore modulate the flux of regolith from hillslope to channel, which in turn modulates the excess transport capacity of the channels and thus their erosion rate.

Topographic Data from LiDAR DEM

To further support our field observation and guide development of a numerical model, we describe data extracted from 1-m LiDAR DEMs of the Book Cliffs and Roan Plateau (Figure 3). Airborne laser swath mapping of 40 km^2 of the eastern Roan Plateau and southern Book Cliffs was conducted in April 2007 using an Optech Gemini Airborne Laser Terrain Mapper, through two seed grants provided by NCALM. Snow was not reported to be present at the time of the survey. NCALM staff used Terrasolid's TerraScan LiDAR software to filter the last returns and generate a 'bare-earth' dataset. After removal of low points and ground classification, DEMs were produced at 1-m spacing using SURFER software, and merged using the Economic and Social Research Institute's (ESRI's) ArcINFO geographic information system (GIS) software. We exported the DEM using ArcMap's Raster Calculator to a RiverTools-compatible grid file.

We used RiverTools software to collect multiple cliff-perpendicular longitudinal channel profiles and cliff-parallel topographic profiles at each location. Drainage area at each grid cell is also calculated using RiverTools software.

Channel profiles and downstream concavity

Profiles of channels that drain the plinth were extracted to provide a representative sample of channel morphology at each location. Due to the jagged nature of the channel profiles at high horizontal resolution (~1 m), before calculating local slope values we smoothed the profiles using an arbitrary fixed vertical interval of 5 m, according to methods described by Wobus *et al.* (2006). We excluded any portion of the vertical cliff (or channel above the cliff) from each profile. We then plotted these channel profile data to determine if they exhibit a power law relationship between drainage area and local slope:

$$S = k_s A^{-\theta} \tag{2}$$

where k_s is referred to as the steepness index and θ is the concavity index (e.g. Snyder *et al.*, 2000; Kirby and Whipple, 2001). Under certain conditions, these regressions can allow one to estimate parameters in the commonly used stream power-based model for bedrock erosion (Howard and Kerby, 1983):

$$E = KA^m S^n \tag{3}$$

If we assume that a river profile is in steady state with respect to climatic and rock uplift conditions, then Equation 3 can be rewritten in the form of Equation 2, to express local slope as a function of drainage area:

$$S = (U/K)^{1/n} A^{-m/n} \tag{4}$$

where U is the rock uplift rate and $(U/K)^{1/n}$ is the channel steepness index, k_s (e.g. Whipple and Tucker, 1999). If the profile is assumed to be in topographic steady state, and the parameters U, K, m, and n are assumed to be uniform, then the concavity index θ may be equal to the m/n ratio (see discussion in Whipple and Tucker, 2002). Some of these assumptions may not be reasonable for the Book Cliffs or the Roan Plateau, given the transient nature of the processes of knickpoint migration and cliff retreat occurring directly adjacent to the plinths. However, this simple analysis allows us to contrast the morphology of the two settings, as a first step towards constraining how processes may also vary between them.

At small drainage areas (less than ~30 000 m^2), channels draining the plinth of the Book Cliffs generally have slope values that are invariant with drainage area and are at or slightly higher than the angle of repose for granular material (~32°). As drainage area increases downstream, however, we observe a power law relationship between channel slope and drainage area (Figure 6), corresponding to channel concavities that range from 0·9 to 1·2 (n=18). Channels draining plinths on the Roan Plateau are generally less concave than their counterparts on the Book Cliffs. For channels draining plinths in canyons on the Roan Plateau, channel slope values are more constant even as drainage area increases. Channels that originate from below the cliff band (that is, with no upstream drainage above the cliff band) have low channel concavities ranging from 0·08 to 0·21. For channels that do have upstream drainage above the cliff band (that is, they access the drainage network of the plateau surface), channel concavities below the cliff band are approximately 0·5.

For the same channel profiles described earlier, we also examined changes in channel width; no significant trends in channel width versus drainage area were found. We extracted topographic profiles perpendicular to the main trend of the channel, and measured channel width as the first clear break in slope above minima in the profile. The 1-m precision of our

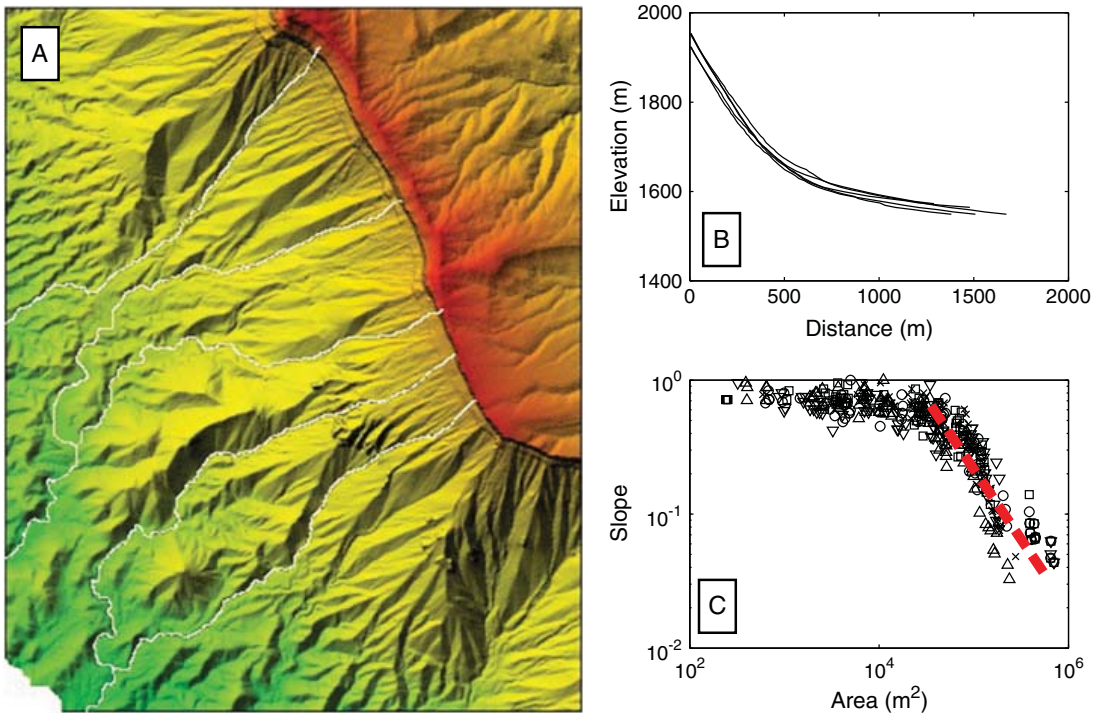

Figure 6. (A) Shaded relief image of portion of ALSM-derived DEM for the Book Cliffs, with five stream channels indicated in white. (B) Stream channel longitudinal profiles. (C) Profile slope versus drainage area, with different symbols corresponding to different profiles. Dashed line indicates concave portion of profiles described in text. This figure is available in colour online at wileyonlinelibrary.com/journal/espl

DEM data restricts our ability to resolve channels that are narrower than a few meters in width. This leads to uncertainty in determining relationships between channel width and drainage area in both field settings.

Channel order and hillslope relief

To describe the relief within the plinth, we drew cliff-parallel topographic profiles spaced approximately 50 m apart down the plinth in each study area. The profiles are several hundred meters to over a kilometer in length, are generally parallel to the strike of the cliffband. We limit the profiles to several hundred meters from the cliff, where the channels draining the plinth tend to flow perpendicular to the trend of the cliff. For the Book Cliffs, we focus our observations on the south-eastern end of the ALSM swath, where the cliffband is single-tiered and less indented (Figure 3). On the Roan Plateau, we limited our observations to areas not affected by natural gas drilling operations.

We see notable differences in transverse hillslope morphology both within and between the two DEMs. On the Book Cliffs, hillslope relief and valley spacing often increase with distance from the cliff, as in the example shown in Figure 7. This change in morphology coincides with an abrupt decrease in the amount of debris cover on the plinth. On the Roan Plateau, no similar change in debris cover appears, and average hillslope morphology measurements are more uniform with distance from the cliff (Figure 8). Profiles on the Book Cliffs tend to exhibit higher hillslope relief relative to valley spacing than profiles on the Roan Plateau. We did not observe a strong control of aspect on Roan Plateau plinth morphology, although aspect has been shown to be important in weathering and erosion processes (e.g. Burnett *et al.*, 2008).

On the Book Cliffs in particular, the increase in hillslope length down the plinth could be related to the integration of the drainage network; higher-order streams are spaced more widely and adjacent hillslopes are correspondingly longer. We expect debris cover to impact this trend. To investigate further, we classified the channel networks extracted from the LiDAR DEMs by Strahler order (Figure 9). We measured the vertical relief between pairs of points chosen arbitrarily from within channels of each stream order and adjacent ridge crests and plotted the relief value against stream order. In the Roan case, the entire plinth is debris-strewn. In the Book Cliffs, we classified each measurement point as belonging to the debris-strewn or debris-free area of the plinth, based on textural differences visible in the DEM and color differences visible in satellite imagery. As could be deduced from the cross-profiles (above), the relief increases little with stream order in the Roan Plateau canyon plinths, where no streams above fourth order are found. In the Book Cliffs, relief increases systematically with stream orders up to six. On the upper, debris-strewn part of the plinth, the relief is markedly more uniform and lower than that in equivalently-ordered streams below, where the debris cover no longer persists. This supports our conceptual model described earlier, which predicts that relief within the plinth should be suppressed where immobile, slow-weathering debris fills channels and covers more weatherable bedrock on the associated ridges.

Hillcrest profile shapes

We also used the LiDAR data to evaluate if hillslopes can be described as parabolic in cross-sectional form, such that slope increases linearly with distance from the hillslope divide. Parabolic morphology is consistent with hillslope lowering by diffusive regolith transport at a comparable rate to that of incision by adjacent channels. Hillslope profiles with steeper-than-parabolic sides indicate that the hillslopes produce sufficient regolith that, in order to remove it from the hillslopes and lower them at the same rate as the channels, slopes must steepen until non-linear-with-slope transport processes (e.g. mass wasting) become active (e.g. Roering *et al.*, 2001).

We applied parabolic curve fits (not shown) to selected segments from the transverse profiles described earlier (Figures 7 and 8), and measured the range in hillcrest curvatures (d^2z/dx^2) if a parabolic shape is assumed. We targeted the uppermost convex portion of each hillcrest, such that curve fit segments contained at least 50 data points in the top 20 m in hillslope elevation. We excluded all curve fits with regression (R^2) values less than 0·9.

Book Cliffs transects have much higher curvatures than do Roan Plateau transects. For plinths on the Book Cliffs, mean hillcrest curvature ranges from –0·007 to –0·019 ($n = 85$). On the

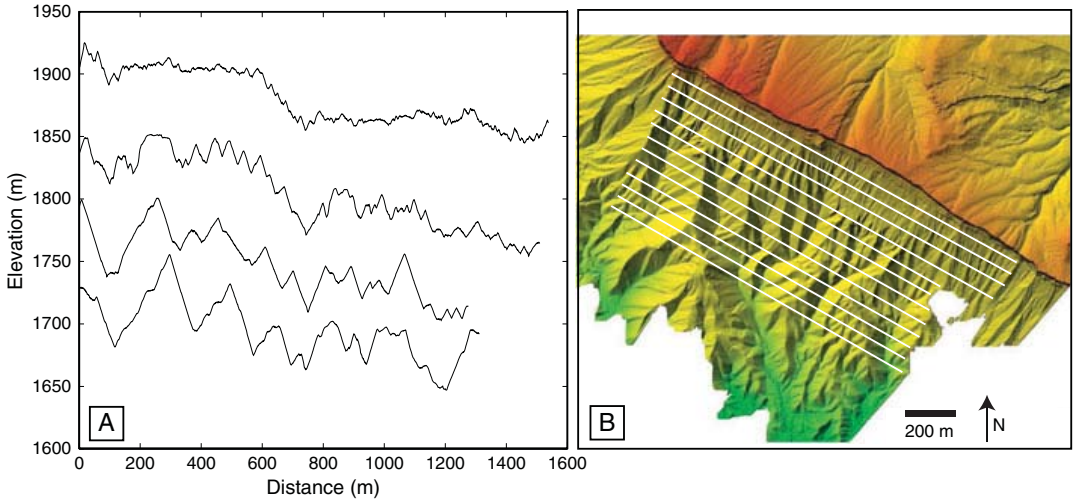

Figure 7. (A) Topographic profiles at approximately 100, 200, 300, and 400 m away from the cliffband on the Book Cliffs. (B) Shaded relief image of ALSM-derived DEM with all profiles indicated by white lines. Across all 12 profiles spanning 600 m in distance from the cliffband, average channel relief increases downslope from ~5 to ~20 m, and average channel spacing increases downslope from ~40 to ~80 m. This figure is available in colour online at wileyonlinelibrary.com/journal/espl

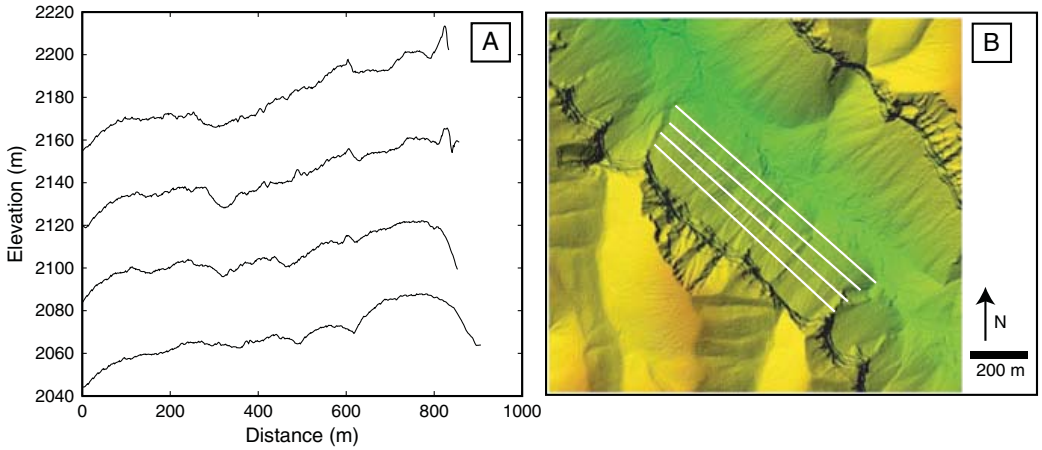

Figure 8. (A) Topographic profiles at approximately 50, 100, 150 and 200 m away from the cliffband on the west side of East Fork Parachute Canyon on the Roan Plateau. (B) Shaded relief image of ALSM-derived DEM with profiles indicated by white lines. Across the profiles shown, average channel relief is relatively stable at ~5 m, and average channel spacing is relatively stable at ~80 m. This figure is available in colour online at wileyonlinelibrary.com/journal/espl

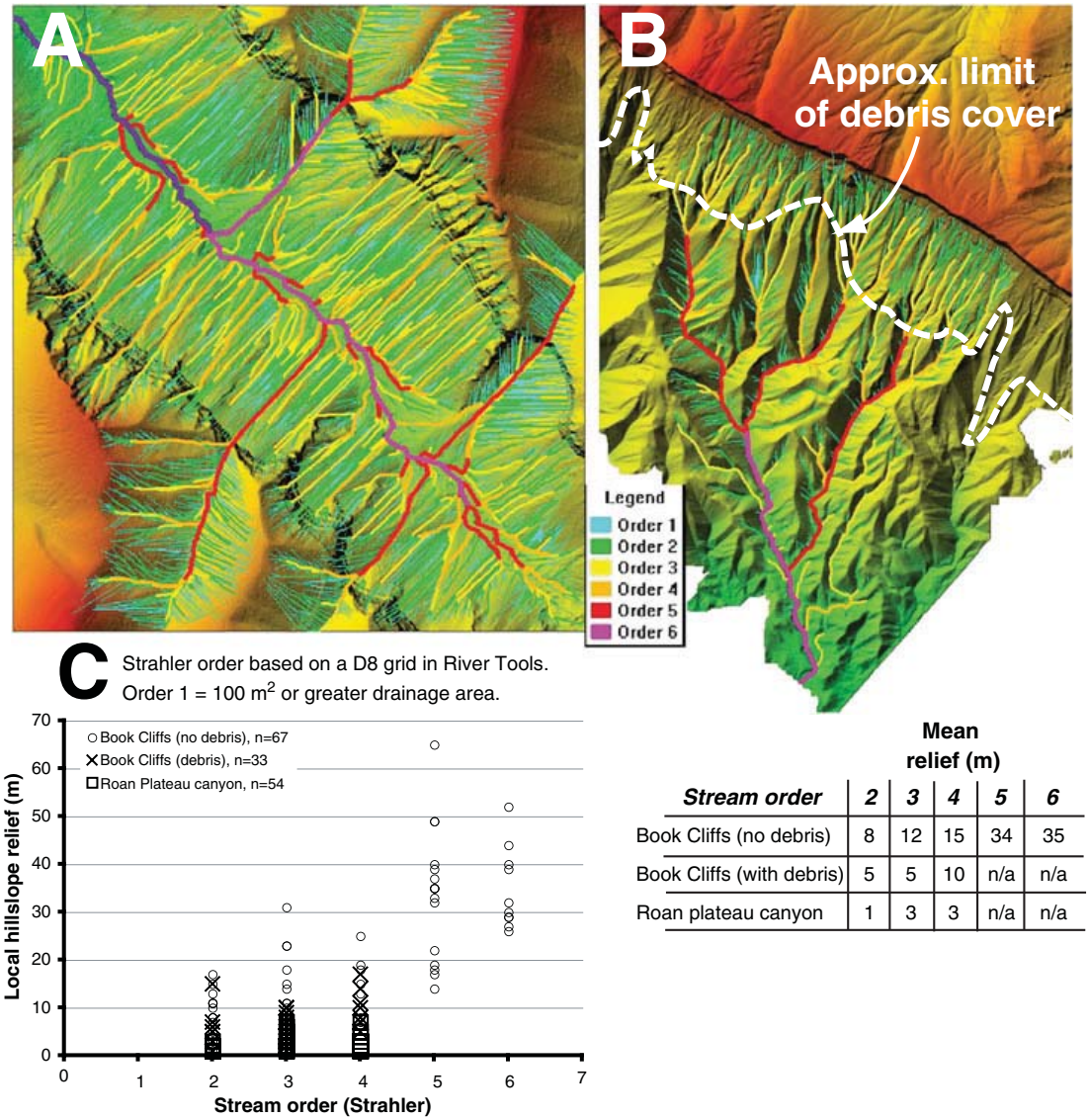

Mean relief (m)					
Stream order	***2***	***3***	***4***	***5***	***6***
Book Cliffs (no debris)	8	12	15	34	35
Book Cliffs (with debris)	5	5	10	n/a	n/a
Roan plateau canyon	1	3	3	n/a	n/a

Figure 9. Strahler order of plinth channels in East Fork Parachute Canyon on the Roan Plateau (A) and the Book Cliffs (B). The upper part of the Books Cliffs plinth is debris-strewn; that in the Roan Plateau is thinly and variably mantled. Hillslope relief (between the channel and the adjacent ridgecrest) increases with stream order in all cases (C), but hillslopes in the debris-strewn areas show less of an increase with stream order and lower overall relief than those developed outside the runout area for rockfall. This figure is available in colour online at wileyonlinelibrary.com/journal/espl

Roan Plateau transects, curvature ranges from –0·0005 to –0·003 ($n = 15$). Moreover, the Book Cliffs profiles are parabolic only through their very uppermost few meters; lower, these hillsides have straight slopes at a consistent angle of 30° to 35° (Figure 7).

The higher relief and curvature of these crosswise hillslopes in the Book Cliffs probably reflect the higher weathering rates of the plinth bedrock. Because these hillslopes are consistently covered with a uniform thickness of regolith, they are probably not detachment-limited. Rather, the soft marine shale here contains shrink-swell clays that cause the rock to disintegrate over a timescale of hours when wet. The lacustrine mudstones of the Roan Plateau, though fissile and pervasively fractured, do not dissolve in water perceptibly over a timescale of weeks. We propose that the Book Cliffs shale hillslopes are steeper to remove the abundantly produced regolith at rates equivalent to local channel incision rates (which may also be higher than those in the Roan Plateau). Specifically, this morphology probably results from a shallow (typically, a few centimeters) landsliding process that one of the authors (R.S.A.) has observed in the field during rain events. The landsliding efficiently transports regolith down slopes of this steepness.

These observations suggest that a non-linear regolith transport rule may better describe the Book Cliffs plinth hillslope processes. Roering *et al.* (2007) present formulae for fitting non-linear transport rules to measured hillslope profiles; however, extraction of meaningful transport parameters from any of these fits (linear or non-linear) requires specific knowledge of local erosion rates, which we have not measured.

Plinth swath profiles

The above sections describe strong differences between the Book Cliff plinth and that of the Roan canyons at the scale of first-order channels. Here we discuss the overall longitudinal profile of each plinth. This 'mean' profile is what characterizes these cliffs when seen from a distance. According to our conceptual model, its slope is adjusted so that the finer-scale processes (those of the intra-plinth drainage system and its hillslopes), working in concert, can transport all regolith produced by weathering the plinth plus that delivered via rockfall from the cliff. In other words, the overall slope of the plinth is set by the generally concave-up channel profiles, but increasing hillslope relief with distance down the plinth results in an overall profile that is markedly straight. From the LiDAR DEMs, we collected swath profiles (as the average of 10 or more individual line profiles drawn perpendicular to the strike of the cliff) to illustrate the mean plinth profile in each setting (Figure 10).

The Book Cliffs swath profiles uniformly steepen about 300 m away from the cliff (Figure 10). The low-slope upper portion of these profiles manifest in map view as an apron that is present throughout the Mount Garfield area. It does not appear to change in width along the escarpment, even as distance to the trunk stream (the Colorado River) increases dramatically to the northwest. The apron's width coincides with the maximum distance that significant amounts of debris were deposited during the June 9, 2009 Palisade rockfall event (see section entitled 'The July 9, 2009 Palisade rockfall') and a change in the amount of debris cover and intra-plinth relief (see section entitled 'Channel order and hillslope relief').

To the southeast, where the Colorado River is close to the base of the cliffs, the entire plinth is shorter than 300 m and is completely debris-mantled. This is the case in the Roan Plateau as well, where the shorter (~300 m long), straighter plinth is completely within the runout zone of the rockfall debris. This suggests the strong role that rockfall debris might have on the overall plinth profile. In settings where the debris does not reach the farther extents of the plinth, the channel-hillslope system there is not perpetually disturbed by the influx of new debris and can establish itself long enough for significant relief to develop.

Numerical Model

We attempt to model in two dimensions the evolution of an escarpment with a single hard caprock layer above a more erodible shale plinth. While striving for simplicity and abstraction, we require a ruleset that (1) conserves mass; (2) forms channel networks and reforms them dynamically as conditions change; (3) represents in some physical way the erodibility differences between rock types; (4) can approximate horizontal cliff retreat on a 2D elevation grid. We must also acknowledge that rockfall debris is prone to accumulation in hollows, channels, and on low slopes, and is not deposited on sharp hillcrests.

To do this, we developed the LEMming landscape evolution model, a 2D, regular-grid, rules-based, hybrid finite-difference/cellular automaton model that is designed to explore the effect of multiple rock types on landscape evolution. LEMming tracks regolith and sediment fluxes, including bedrock erosion by streams and rockfall from steep slopes. With this model we explore the coupling between the bedrock channels and regolith-mantled hillslopes of the shale plinth and the sandstone cliff above.

The Appendix contains a detailed description of the LEMming model. In brief, the model represents stochastic failure of a sandstone cliff above a fluvial landscape carved into more erodible rock. Model grid cells with slope angles above a threshold, and which correspond to the appropriate rock type, are designated as candidate sources for rockfall. Rockfall erosion of the cliffband is simulated by instantaneously reducing the height of a randomly chosen grid cell that is susceptible to failure to that of its nearest downhill neighbor among the eight cells bordering it. This volume of rockfall debris is distributed across the landscape below this cell according to rules that weight the likelihood of each downhill cell to retain rockfall debris. The weighting is based on local conditions such as slope angle, topographic curvature, and distance and direction from the rockfall source. Rockfall debris and the bedrock types are each differentiated by the rate at which they weather to regolith and by their fluvial erodibility. Regolith is moved according to transport rules mimicking hillslope processes (dependent on local slope angle), and bedload and suspended load transport (based on stream power). Regolith and sediment transport are limited by available material; bedrock incision occurs (also based on stream power) where bare rock is exposed.

It may be possible to find geomorphic transport laws (in the sense of Dietrich *et al.*, 2003) that express quantitatively each of these processes over the range of slope conditions, grain sizes, erosion rates, and water flow conditions found in these very steep escarpments, but we are unaware of any presently in use that are directly applicable to this setting. We therefore use a general ruleset that mimics the behavior of specific components of the cliff-plinth system, in order to explore how these components interact to determine cliff morphology and retreat rate. Given this, our parameter values are chosen to produce the desired behavior and have no direct physical meaning, but the response of the modeled system (the

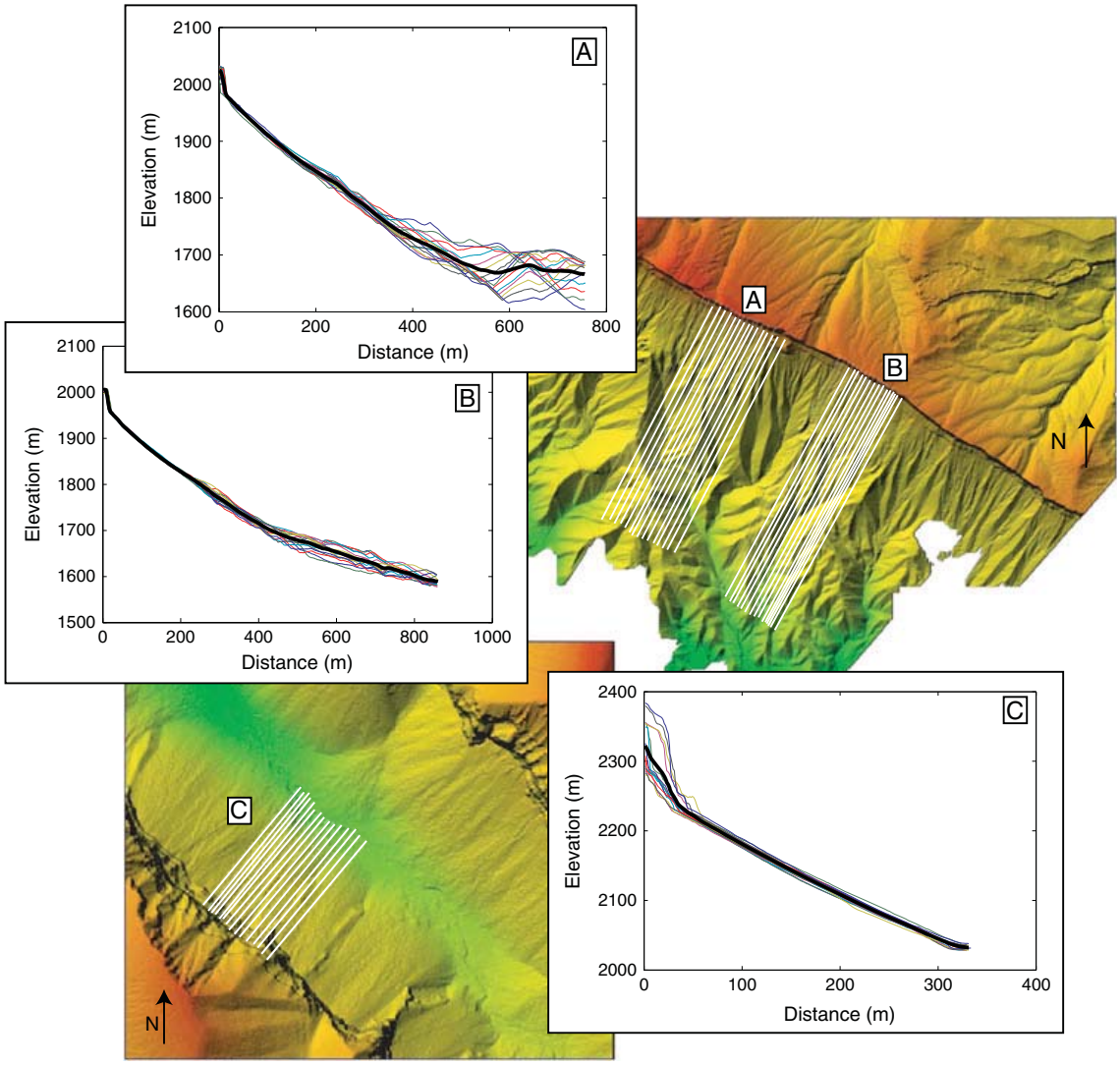

Figure 10. Longitudinal swath profiles down the Book Cliffs (A, B) and Roan Plateau (C) plinths. Note the break in slope about 300 m from the cliffband in the Book Cliffs, coinciding with the runout distance of rockfall debris. The entire plinth in the Roan Plateau is within the runout distance, and no break in slope is manifest there. This figure is available in colour online at wileyonlinelibrary.com/journal/espl

interaction of the rules) to relative changes in these values is nonetheless an informative approximation.

Modeling Experiments

Rather than attempting to tune our model to precisely match a particular landscape (which, given the abstracted transport ruleset, would be uninformative), we generalize by experimenting on a 500-m escarpment with a 50-m thick sandstone caprock (Figure 11). We establish a base parameter set that is held constant across all model runs, and vary only one parameter of interest for each of a limited set of experiments. In the experiments described here, we focus on the linkage between cliff retreat and plinth downwearing, specifically targeting the influence of rockfall debris on cliff morphology and retreat rate.

Here we describe two model scenarios that illustrate the effect of plinth dynamics and rockfall debris on the morphology and retreat rate of escarpments. Tables II and III list the relevant model parameters and their typical values; Table IV lists the parameters and values modified for each experiment. In all model runs we employed a timestep of one year and a grid spacing of 10 m.

Scenario 1: Varying weathering rate of debris to regolith

In this set of experiments, we explore the influence of rockfall debris properties on the morphology and retreat rate of the model escarpment. The rate of cliff retreat by rockfall is not externally limited, but is regulated by the rate at which the cliff face is steepened by plinth erosion. The experimental variable is the rate at which rockfall debris breaks down to regolith, which can then be removed by fluvial and hillslope transport. We vary this parameter from 1 m/yr to 10^{-6} m/yr in each of two sets of runs; between each set, the rate of regolith production from the plinth bedrock varies by a factor of 10 (0·001 m/yr, runs 1-a through 1-h; and 0·01 m/yr, runs 1-i through 1-p; see Table IV).

Scenario 2: Varying restriction on rockfall backwearing rate

In this scenario, we simulate a setting in which the rockfall rate is externally controlled by climate, hydrology, or lithology, and

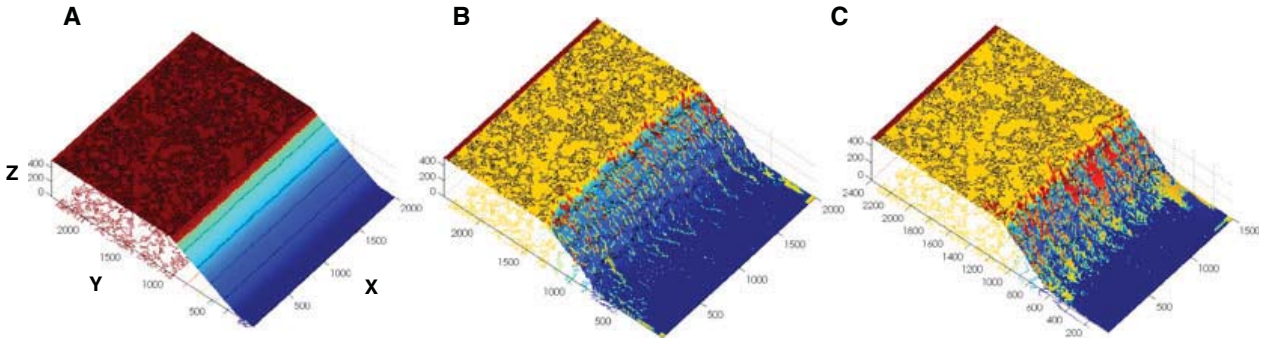

Figure 11. Example model landscapes showing rockfall debris. Different colors indicate rocktype; shading is by elevation; 100 m contours. (A) Universal initial condition. Caprock is 50 m thick. (B) 200 kyr snapshot of run 1-d, debris weathering rate 0·005 m/yr. Note the debris is mostly contained within the channels on the plinth. (C) 200 kyr snapshot of run 1-f, debris weathering rate 10^{-4} m/yr. The decreased weathering rate of the debris has allowed it to accumulate, mantling hillslopes to a greater degree. This figure is available in colour online at wileyonlinelibrary.com/journal/espl

Table II. LEMming universal input parameters[a] and default values

Parameter	Value	Unit	Description
Grid size			
x	200	pixels	Landscape size *(X)*
y	240	pixels	Landscape size *(Y)*
dx	10	m	Grid cell size
dy	*dx*		
Timesteps and model duration			
dt	1	yr	Timestep
tmax	4·00E+05	yr	Model run duration
Physical parameters			
rock_uplift	0	m/yr	Rock uplift rate relative to grid boundary
stream_width_coeff	0·01	—	Multiplies the width = sqrt(area) function.
Regolith properties			
kappa	0·1	m/yr	Regolith transport coefficient (m/yr)
sc	inf	m/m	Critical slope above which diffusion is non-linear with slope
kt	0·001	1/(m/yr)	Fluvial bedload transport efficiency
mt	1	—	Area exponent on fluvial bedload transport equation
nt	1	—	Slope exponent on fluvial bedload transport equation
Max_Mobile_H	0·05	m	Maximum thickness of mobile layer of regolith
Suspended sediment			
ArDL	7·00E+04	m^2	Reference area at which suspension slope is defined
SrDL	0·1	m/m	Slope at which entire mobile thickness of sediment moves in suspension given the reference drainage area
Rockfall parameters			
RFSource_curv	0	1/m	Curvature below which qualifies a rockfall source (universal − threshold slope is set by rock type)
Backwearing_Rate	inf	m^3/yr	Backwearing erosion rate cap on rockfall, per meter of horizontal cliff length
Rockfall debris distribution			
DepoAngleCutoff	30	deg	Azimuthal angle from source surface normal beyond which deposition probability is zero
distStar	100	m	e-folding lengthscale (in meters) for falloff of deposition with distance
distMax	inf	m	No deposition allowed more than this far from a source
curvStar	0·25	1/m	Approximate curvature where deposition probability asymptotes to zero (when −) and one (when +)
slopeExp	1	—	Deposition falls off as 1/slope^slopeExp
sDepCrit	1·1	m/m	Above this slope deposition probability is zero.

[a]See Table III for properties defined by rock type.

not by the rate at which the cliff is undermined. We wish to know whether a steady plinth morphology appears in these rockfall-limited cases in order to transport the steadily supplied rockfall debris. We limit the rockfall rate so that only a certain volume of rockfall erosion may occur in a model year. This effectively regulates the rate of cliff retreat. We vary this rate over two-orders of magnitude, again in two sets of runs: (1) runs 2-a and 2-b have debris properties identical to those in run 1-c; and (2) runs 2-c to 2-k have debris with identical properties (both fluvial erodibility and weathering rate) to the shale, or plinth bedrock (see Table IV).

Model Results

The timescale for adjustment from initial condition for each run can be determined by the decrease and leveling-off of

Table III. LEMming rocktype input parameters and default values[a]

Parameter	Value	Unit	Description
Rocktype 0 – default substrate			
k0	5·00E−06	1/(m/yr)	Fluvial erodibility constant
m0	1	—	Stream power area exponent
n0	1	—	Stream power slope exponent
rdot0	*0·01*	*m/yr*	*Bare-rock regolith production rate*
rstar0	0·01	m	e-folding depth for falloff of regolith production
rfslope0	inf	m/m	Positive slope above which qualifies a rockfall source ('threshold slope')
Rocktype 1 – caprock			
k1	1·00E−07	1/(m/yr)	Fluvial erodibility constant
m1	1	—	Stream power area exponent
n1	1	—	Stream power slope exponent
rdot1	1·00E−06	m/yr	Bare-rock regolith production rate
rstar1	0·003	m	e-folding depth for falloff of regolith production
rfslope1	3	m/m	Positive slope above which qualifies a rockfall source ('threshold slope')
Rocktype 2 – rockfall debris			
k2	*1·00E−07*	*1/(m/yr)*	*Fluvial erodibility constant*
m2	1	—	Stream power area exponent
n2	1	—	Stream power slope exponent
rdot2	*0·01*	*m/yr*	*Bare-rock regolith production rate*
rstar2	0·1	m	e-folding depth for falloff of regolith production
rfslope2	inf	m/m	Positive slope above which qualifies a rockfall source ('threshold slope')

[a]Parameters in italics varied as part of experimental runs; see Table IV.

Table IV. Experimental input parameters[a]

Parameter:	Rocktype 0 – plinth rock regolith production rate (m/yr) rdot0	Rocktype 2 – rockfall debris fluvial erodibility (1/m/yr) k2	Rocktype 2 – rockfall debris regolith production rate (m/yr) rdot2	Backwearing erosion rate cap on rockfall (m^3/yr per m cliffline) backwearing_rate
Scenario 1				
Run number				
1-a	0·01	1.00E—07	1	inf
1-b	0·01	1.00E—07	0.1	inf
1-c	0·01	1.00E—07	0.01	inf
1-d	0·01	1.00E—07	0.005	inf
1-e	0·01	1.00E—07	0.001	inf
1-f	0·01	1.00E—07	1.00E-04	inf
1-g	0·01	1.00E—07	1.00E-05	inf
1-h	0·01	1.00E—07	1.00E-06	inf
1-i	0·001	1.00E—07	0.1	inf
1-j	0·001	1.00E—07	0.01	inf
1-k	0·001	1.00E—07	0.008	inf
1-l	0·001	1.00E—07	0.005	inf
1-m	0·001	1.00E—07	0.001	inf
1-n	0·001	1.00E—07	5.00E-04	inf
1-o	0·001	1.00E—07	1.00E-04	inf
1-p	0·001	1.00E—07	1.00E-05	inf
Scenario 2				
Run number				
2-a	0·01	1.00E—07	0.01	0.5
2-b	0·01	1.00E—07	0.01	0.05
2-c	0·01	1.00E—06	0.01	0.5
2-d	0·01	1.00E—06	0.01	0.4
2-e	0·01	1.00E—06	0.01	0.3
2-f	0·01	1.00E—06	0.01	0.25
2-g	0·01	1.00E—06	0.01	0.2
2-h	0·01	1.00E—06	0.01	0.15
2-i	0·01	1.00E—06	0.01	0.1
2-j	0·01	1.00E—06	0.01	0.05
2-k	0·01	1.00E—06	0.01	0.005

[a]Only parameters that differ from the base values (Tables II and III) are listed for each experiment.

volumetric fluvial erosion rates, a quantity tracked by the model. This timescale depends mostly on the erodibility and weathering rate of the plinth rock, because most of the adjustment happens before rockfall debris significantly covers the plinth. We did not vary the fluvial erodibility of the plinth bedrock between any of the model runs; we did vary its

weathering rate by one order of magnitude. For the runs with high weathering rate (0·01 m/yr), the fluvial sediment output stabilizes around 10 kyr; for the lower rate (0·001 m/yr), the adjustment timescale is ~25 kyr. All averaged retreat rates that we report are measured over a period beginning at least 100 kyr into the run, so that this initial period of adjustment is not included (i.e. we ignore the 'spin-up' period). Figure 12 illustrates example model output from 100 kyr in the different scenarios.

Scenario 1 results – debris weathering rate

Retreat rates

Summarized in Figure 13, the mean rates of cliff retreat (measured at the top of the cliff in 200-m wide swath profiles located in the center of the model domain) are a non-linear function of the rate at which debris weathers. As the debris weathering rate is decreased below that of the plinth rock, the overall cliff retreat rate falls off quickly at first, then more gradually as the contrast becomes more extreme. We attribute this non-linearity to two related effects: as debris becomes harder, it takes longer to remove; in addition, the percent of the plinth area that it covers increases so its effect becomes stronger. When the debris weathering rate is two or more orders of magnitude slower than that of the plinth rock, the plinth becomes completely mantled, additional rockfall is stifled because the cliff is no longer being undercut, and cliff retreat essentially shuts down.

In runs 1-a through 1-c, the debris weathers more quickly than the plinth bedrock and overall retreat rates do not depend on the debris weathering rate. The debris is evacuated rapidly enough that it does not significantly affect the retreat of the escarpment. In contrast, runs 1-i through 1-p were performed with plinth bedrock that weathered 10 times more slowly. Because of the lower rate of regolith production from plinth bedrock, relief on the plinth is correspondingly lower. This lower relief can be completely filled by rockfall debris and the regolith it produces. For this reason, in these runs, the escarpment retreat rate is affected by debris even when the debris weathers much more rapidly than the plinth rock (Figure 13A, gray squares). This 'swamping' effect illustrates the complex interplay between the lithologies present on the plinth, with the plinth bedrock properties affecting the efficiency by which rockfall debris can be evacuated.

Morphology

When the plinth becomes completely mantled with rockfall debris, its slope angle adjusts to transport this debris given its erodibility and weathering rate. When the debris is more difficult to erode fluvially than the plinth bedrock, detachment-limited channels tend to steepen, thus steepening the overall plinth profile (Figure 14). Meanwhile, the reduced regolith supply from debris that weathers slowly tends to reduce crosswise relief, resulting in a more planar plinth. Depending on the horizontal length of the plinth, there may be a break in slope associated with the extent of debris cover. In cases where the plinth is longer than the rockfall runout distance and the rockfall debris is slower to weather than the plinth rock, a compound slope develops (e.g. Figure 12B). Portions of the Book Cliffs display this compound-slope morphology (Figure 10).

In cross-section, plinth relief is most strongly affected by the competition between weathering rate of the plinth rock and its fluvial erodibility. As the rate of the shale bedrock weathering increases, so does the cross-profile relief, because (holding the channels constant) the hillslopes must steepen to transport the additional regolith. For debris weathering rates that are higher than those of the plinth rock, crosswise relief is little affected by the presence of debris (Figure 15). As debris weathering rate is reduced, coverage increases, reducing the amount of available regolith and allowing relief to decline. At very high contrasts in weathering rate, debris acts as an effective long-term armor for the plinth rock, prompting runoff to cut new channels into the softer rock around these areas of debris. This causes the topography to invert. Erosion rates of the relic debris-capped surfaces decline further as they are progressively abandoned by the streams, and relief between their surfaces and the adjacent valleys can grow to hundreds of meters as the valleys tap escarpment area behind the abandoned surface (Figure 15).

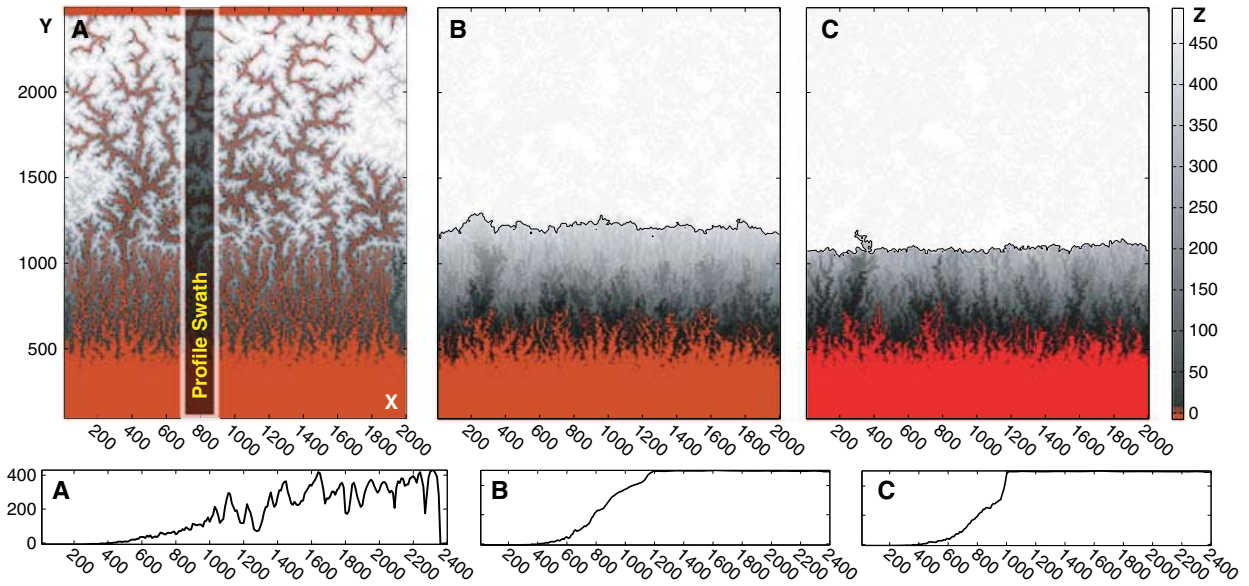

Figure 12. Example model output from 100 kyr., with map view (top) and longitudinal swath profiles (bottom). (A) Control run in which the caprock is identical to the underlying plinth bedrock. Note the extensive dissection. (B) Run 1-d; moderate debris weathering rate and no limit on rockfall backwearing rate. (C) Run 2-j; backwearing rate by rockfall restricted to 0·05 m^3/yr per m cliffline. This figure is available in colour online at wileyonlinelibrary.com/journal/espl

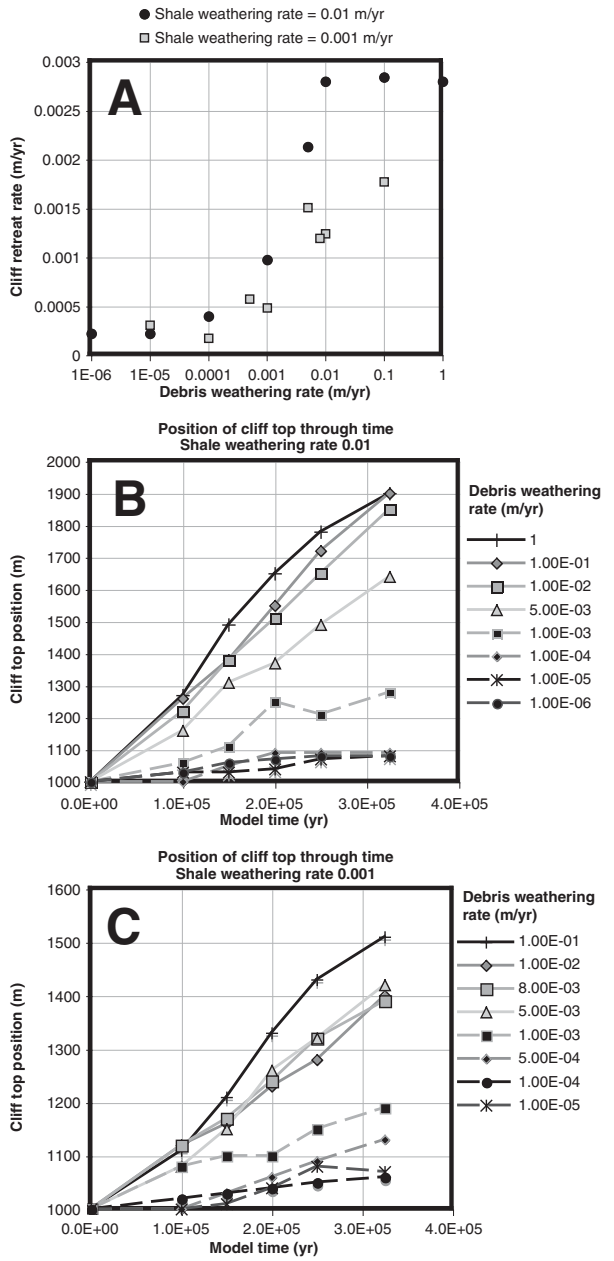

Figure 13. Retreat rates and histories for Scenario 1 runs. (A) Runs 1-a through 1-h (black circles); Runs 1-i through 1-p (gray squares). (B) Runs 1-a through 1-h. (C) Runs 1-i through 1-p.

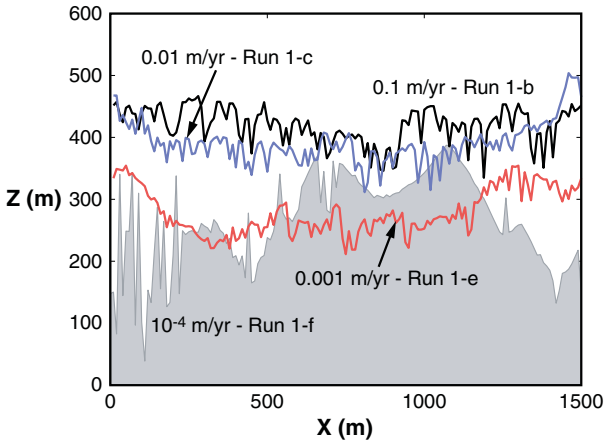

Figure 15. Plinth cross-profiles for select Scenario 1 model runs at 300 kyr. Profiles drawn parallel to the cliffband, 250 m down the plinth from the cliff. Top to bottom – decreasing weathering rate of debris. Bare-rock weathering rate of plinth bedrock is 0·01 m/yr throughout. More slowly weathering debris results in greater debris coverage and less regolith, reducing small-scale relief, but increases broader-scale topographic variability by armoring portions of the plinth. Shaded profile from Run 1-f illustrates topographic inversion. Cf. Figures 7, 8. This figure is available in colour online at wileyonlinelibrary.com/journal/espl

Dynamic behavior

Under certain model conditions (e.g. runs 1-d and 1-e), debris accumulation fills in the upper portions of channels and creates areas of lower slope and relief on the plinth. These 'flat spots' are more favorable (according to our model criteria) for debris accumulation than downslope areas, and so tend to trap rockfall debris and grow in area. This feedback causes these debris fields to expand rapidly (over a few thousand model years) until they partially cover the plinth; once large enough, they inhibit downwearing of the plinth and rockfall is shut down along the corresponding section of the cliff. No longer supplied continuously with new material, the debris fields erode away as quickly as they formed.

This dynamic behavior only occurred in model runs where the debris weathered slightly less rapidly than the plinth rock. When debris was much slower to weather, it ended up mantling the entire plinth, shutting down rockfall overall and behaving more as capping bedrock than as sediment. In runs where the debris weathered and eroded more quickly than plinth bedrock, it did not accumulate significantly. These internal dynamics can be seen in the retreat rate plot for the Scenario 1 runs with intermediate debris weathering rates (Figure 13). Retreat rates in these instances, although predictable in the long term, exhibit more temporal variability than in the cases of very low or very high debris weathering rates.

Scenario 2 results – limited cliff backwearing rate

Retreat rates

In this scenario we prescribed the volumetric limit on rockfall, thereby prescribing the overall retreat rate of the cliff. The

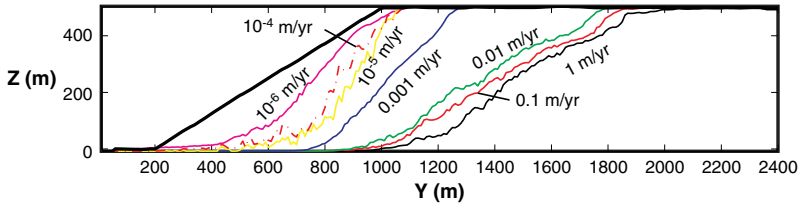

Figure 14. Longitudinal swath profiles for different Scenario 1 model runs at 300 kyr: Heavy black line – initial condition; remainder, left to right – increasing weathering rate of debris. Bare-rock weathering rate of plinth bedrock is 0·01 m/yr throughout (runs 1-a through 1-h). The steeper profiles correspond to a greater degree of mantling by debris. See Figure 12 for swath location. This figure is available in colour online at wileyonlinelibrary.com/journal/espl

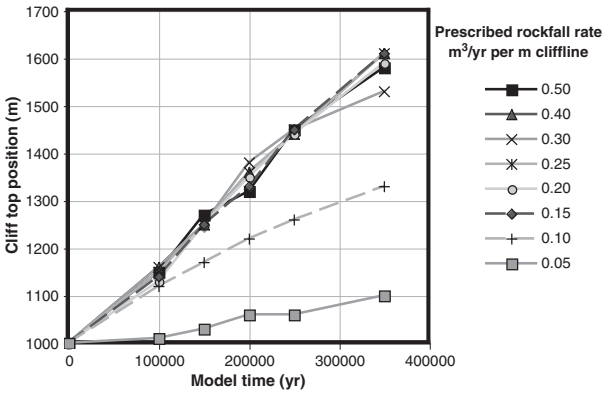

Figure 16. Retreat histories for Scenario 2 runs. For prescribed rates of rockfall erosion greater than 0·15 m^3/yr per m cliffline, retreat rates are the same, implying internal rate limitation.

retreat histories for the different runs are shown in Figure 16. In these runs, for high prescribed rockfall rates (≥0·15 m^3/yr per m cliffline), the retreat rates were identical; the system was not reaching our prescribed limit because not enough new rockfall sources were available each timestep. In other words, erosion of the plinth was not fast enough in these cases to trigger rockfall at the prescribed rate, and thus the cliff retreat rate was internally limited.

In the case of lower prescribed rates, the plinth wasted away and, after sufficient time, the system evolved into a vertical cliff with no plinth, continuing to retreat at the prescribed rate. The rate at which the plinth wastes away depends on the strength of processes that act on it. The lower the cliff retreat rate we specify, the sooner the plinth is gone, reduced only to a pile of rubble at the base of a vertical cliff.

Morphology

Lengthwise and crosswise plinth morphologies evolve as they do in the soft-debris cases of Scenario 1. In the swath profiles (Figure 17), the upper break in slope is seen throughout the runs, until (in cases of plinths that waste away), the plinth is short enough that it receives relatively uniform debris cover. At this point, the plinth profile becomes very straight, as in the plinths in canyons on the Roan Plateau.

None of the prescribed-backwearing model runs we performed reached a steady morphology with a short plinth. This would require that, after some plinth downwasting, the plinth erosion came into perfect balance with the cliff backwearing. It is possible we could produce this behavior using slower-weathering debris – for most of the Scenario 2 runs, rockfall debris had the same properties as the shale. The only runs we did with slower-weathering debris in this vein (runs 2-a and 2-b) also generated either a vertical cliff or a segmented escarpment, implying that even in cases of slow-weathering debris, only a very narrow range of externally limited cliff backwearing rates would perfectly balance plinth erosion to make a steady plinth profile under a tall cliff.

Discussion

Our numerical model codifies our conceptual model and successfully reproduces several features of the escarpments shown in Figure 1 and described in the sections entitled 'Field Areas' and 'Topographic Data from LiDAR DEM': crosswise hillslopes on the plinth; inverted topography; debris-filled channels; a segmented plinth; and a relatively straight cliffline in planview. Although the different aspects of plinth morphology represent a conspiracy of several processes interacting in a complicated way, we can generalize the dominant controls on each (Table V). Crosswise relief within the plinth appears to be controlled by the production rate of regolith on the plinth from bedrock and rockfall debris. The slope of the longitudinal profile of the plinth appears to be more strongly controlled by the long profiles of the streams, reflecting their ability to remove regolith and to incise the bedrock or rockfall debris directly. A segmented plinth develops where rockfall is actively replenishing the debris fields and stochastically interrupting channel formation. When rockfall debris that is sufficiently slow to weather fills channels, it can armor them and produce inverted topography; in the extreme cases, we observed one-pixel 'earth pillars' and long, branching mesas that formed by inversion of plinth channels as the escarpment retreated.

Commonly, the vertical cliff extends below the base of the caprock in our model simulations, consistent with observations in the field. This results from the incision of the plinth by channel headwaters and lowering of plinth hillslopes by weathering and regolith transport. In those models in which

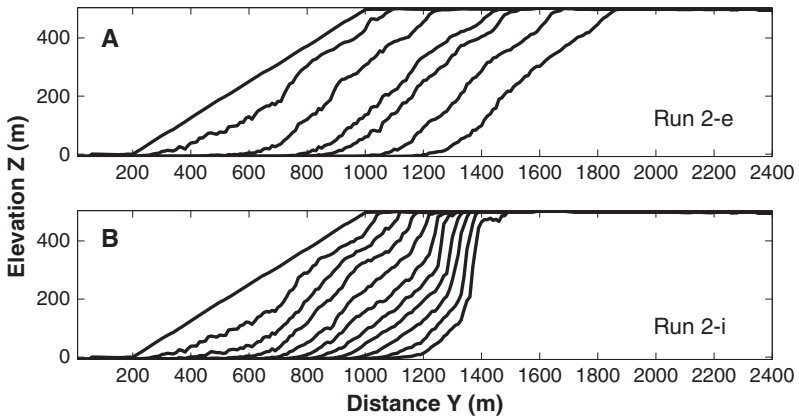

Figure 17. Swath profiles drawn at 50 kyr intervals during two Scenario 2 model runs. (A) High allowed rockfall backwearing rate (0·3 m^3/yr per m cliffline). (B) Lower allowed backwearing rate (0·1 m^3/yr per m cliffline). Limiting the retreat of the cliff promotes downwearing of the plinth. Note in both runs the segmented plinth slope, with a break around 300 m from the cliff; in (B), as the plinth's horizontal length decreases below 300 m, it becomes a single straight slope. Approximately 90% of the rockfall debris should accumulate within 300 m of the cliff given the deposition rules in the model.

Table V. General effects of model parameters on cliff-plinth morphology

Change	Result	Morphology
Decrease weathering or transport rate of rockfall debris	Increase residence time and coverage area of debris on plinth; reduce stream incision rates	Reduced local relief and a straighter longitudinal plinth profile within affected area of the plinth; if this is not the entire plinth, a segmentation between the upper debris-strewn plinth and the lower debris-free plinth may develop
Limit rockfall backwearing rate	Lower coverage of debris on plinth	Plinth lowers, increasing cliff height. Eventually results in removal of the plinth.
Increase weathering rate of plinth bedrock	Transport limitation of hillslope erosion	Increased slope and relief of hillslopes within plinth
Increase incision rate of bedrock channels	Transport limitation of hillslope erosion	Increased slope and relief of hillslopes within plinth

we did not specify a backwearing rate, the rate-limiting factor for cliff retreat was the triggering of rockfall by growth of the cliff face height. This is supported by the general uniformity of cliff heights along escarpments. We did not explore the specific physics by which a taller cliff leads to a greater likelihood of rockfall.

We might expect that continuous reorganization of the channels on the upper part of the plinth due to stochastic rockfall input would inhibit development of permanently located, deeper channels. These permanent channels are those that would promote alcoving of the cliffline by increasing cliff height at their tips; continual debris input should therefore tend to maintain a straight cliffline. Shallow alcoves developed in most model runs, but overall the cliffline never became deeply indented. It is possible that our model domain did not include a long enough portion of cliffline for such alcoving to become apparent. Alternatively, alcoving may depend more on the properties of the caprock (which we did not vary) than on plinth processes. For example, variability in the backwearing rate due to variation in material properties along a cliffband can significantly impact the planview morphology of the escarpment (Howard, 1995). Additionally, we ignored the importance of joint orientation on rockfall, which has been shown to strongly influence cliff retreat rate (e.g. Howard and Selby, 1994; Moore *et al.*, 2009) and could introduce an anisotropic flavor to the development of the planview topography.

We modeled only a single caprock layer for simplicity, but in nature many escarpments have multiple cliff-forming units among more erodible rocks. A potential future target for this kind of model is to consider the effects of stacking these cliff-plinth systems, particularly among dipping stratigraphy, which impacts the planview form of the Book Cliffs (see section entitled 'Book Cliffs') as well as the upper 'relict' landscape above the canyons of the Roan Plateau (Berlin and Anderson, 2009). The staircase in such iconic landscapes as Marble Canyon (Figure 1D) could then be assessed.

Grainsize effects are challenging to represent physically on a numerical grid with a 10-m or even a 1-m spacing. On many talus slopes, rockfall debris is subject to a pronounced size sorting, such that the largest boulders can roll farther downslope than smaller debris (e.g. Pérez, 1989, and references cited therein). These boulders might preferentially lodge in channels, whereas smaller debris might stop readily on unchanneled hillslopes, affecting the spatial pattern of surface armoring and promoting topographic inversion. Large boulders persist longer and may be reworked many times, toppling from ridge to channel. Smaller debris can be carried off the plinth more quickly and might weather more quickly as well. Broad spatial variations of grainsize could nonetheless be approximated in our current model by spatially varying the weathering rate of rockfall debris or the transport coefficient of regolith it generates; however, we did not test its effects because we suspect it would have a secondary impact on plinth morphology and cliff retreat rate.

Influence of climate

Climate could impact the cliff-plinth system in a number of ways. Altering the relative weathering rates of debris and plinth bedrock could have a significant impact on retreat rates. Specifically how precipitation and temperature affect regolith production rates depends on the lithologies involved. For a given change in climate, debris cover on some escarpments could increase, slowing retreat, while debris cover on others could decrease and cause the retreat rate to increase. Important – but difficult – numbers to quantify, then, are the weathering rates of rockfall debris and the plinth rock. Moreover, changing climatic conditions might lead to changes in rockfall recurrence through time, because the relative strengths of processes such as groundwater sapping, frost cracking, root cracking, and surface runoff depend on temperature and precipitation levels.

Climatic changes might also prompt base level changes by enhanced incision of trunk streams near an escarpment. For example, near the Caineville Mesa escarpment (the Blue Hills Badlands of south-eastern Utah), terraces on the Fremont River have been interpreted as forming during hiatuses in downcutting related to glacial–interglacial variations in sediment supply (Repka *et al.*, 1997). Various debris-capped 'mesas' within the badlands appear to grade to these terrace levels, and appear to have been abandoned when a wave of incision propagated up from the Fremont River following a terrace-forming epoch (Gilbert, 1877; Howard, 1997).

In regions where no such base-level control has been documented, our modeling offers an alternative explanation for the formation of debris-capped surfaces on the plinth. Development of a flatter, debris-strewn upper plinth and higher-relief lower plinth can occur solely by limiting the rockfall debris runout distance to the upper portion of the plinth, thus requiring a different adjustment of channels and hillslopes there to transport the regolith produced from this debris. In this case, no change in base level is required.

Yet another potential effect that climate could have on plinth morphology is through promotion or discouragement of vegetative growth on the escarpment. Indeed, on both the Book Cliffs and in the canyons of the Roan Plateau, some of the older debris fields are grass-covered and stable against fluvial erosion even though most of the coarse debris in the field has significantly weathered. Stabilization by vegetation would be equivalent to locally decreasing the regolith transport efficiency in the model; by analogy with Equation 1, reducing the

transport efficiency k results in a corresponding increase in hillslope relief, assuming that the adjacent streams continue to incise at a constant rate.

Because of the multiplicity of climatic effects discussed earlier, and their potential to yield offsetting effects, it is difficult to generalize (for example) that a precipitation increase will always increase the backwearing rate of an escarpment; more efficient fluvial incision of the plinth might be offset by stabilization of hillslopes by vegetation. The ultimate response to a given climate change will depend not only on the magnitude and direction of the change but also on the context: lithologic controls on weathering rate; hydrology; active transport processes; and indeed, the baseline regional climate.

Conclusions

Straight bedrock plinths that lie beneath vertical cliffs are common features of the Colorado Plateau and many other arid landscapes. We argue that any given longitudinal slice of the plinth may operate as both a hillslope and a channel at different points in time. Using a 2D numerical model to simulate the evolution of a retreating escarpment, we have shown that the quantity and quality of debris supplied to the plinth from cliff retreat can disrupt channelization and reduce the lowering rate of the plinth, affecting its internal morphology as well as its overall profile. The commonly observed cliff-plinth morphology arose in our model for all cases in which the cliff retreat rate was limited by the downwearing rate of the plinth at the cliff base; when rockfall rates were externally limited, the plinth disappeared over the course of a few hundred thousand model years.

Introducing debris that is more resistant to erosion than the underlying bedrock can bury existing channels, reduce relief, and lead to inverted topography. This is consistent with our field observations. Under certain conditions, dynamic auto-cyclic behavior can arise on these escarpments without a change in external forcing. This can generate morphologies that could be interpreted as reflecting such external changes (e.g. base-level fall, climate-induced changes in weathering rates, change in rainfall on the escarpment, and so forth), but are simply manifestations of the stochastic delivery of rockfall debris to the plinth and the interaction between this debris and the fluvial network. Perhaps of broader importance, the erodibility of this debris can very strongly impact (10-fold or greater) escarpment backwearing rates. When considering the retreat of these escarpments, even at broad scales, the lithologies of the stratigraphic units and the debris shed from them cannot be ignored.

Acknowledgements—We thank the National Center for Airborne Laser Mapping for providing data, and the National Science Foundation for providing funding (grant #EAR-0545537 to RSA). Thanks also to Nate Bradley for assistance in the field and discussions. We thank two anonymous reviewers and the editor and special issue editor at ESPL, whose comments were extremely helpful.

Appendix: Numerical model description

The LEMming model is similar in many ways to other 2D landscape evolution models (such as GOLEM (Tucker and Slingerland, 1997), CHILD (Tucker *et al.*, 2001), Howard's (1994) drainage evolution model, and ZScape (Densmore *et al.*, 1998)). In contrast with most of these, it was designed from the ground up to incorporate arbitrary stratigraphy and to represent differences in rocktype in a straightforward, physical way. LEMming will be made available via the Community Surface Dynamics Modeling System (http://csdms.colorado.edu) concurrent with publication of this manuscript.

Drainage calculations

Channel slopes and contributing areas are calculated initially and recalculated each timestep using the D_∞ algorithm of Tarboton (1997), which does not force flow from each pixel into only one neighboring pixel and thus does not artificially enhance or inhibit convergent or divergent flow, while remaining computationally efficient. Following Howard (1994), we approximate stream width (W) as:

$$W = c_1 A^{1/2}, \tag{A1}$$

where c_1 is a parameter and A is the D_∞ upstream area. This width as a fraction of the grid spacing corrects stream power for stream widths that are smaller than the model grid spacing and eliminates one source of resolution-dependence in the model. As we describe in the section entitled 'Channel profiles and downstream concavity', it was not possible to extract meaningful channel width data from the LiDAR DEMs, so the width function used here was parameterized arbitrarily and held constant across all model runs.

Bedrock incision

We use a stream-power-like, detachment-limited bedrock incision rule (e.g. Equation 3). This rule is applied at each cell whose regolith thickness is zero for part or all of a timestep. Because in the Book Cliffs, the small first-order channels are generally cut into the shale bedrock and are limited in their transport of larger sandstone debris by the rate at which it weathers to sand, they are effectively detachment-limited throughout, with the sandstone debris acting as bedrock. Thus, the 'cover effect' is modeled by applying the bedrock incision rule at a cell only during the fraction of each timestep over which the regolith thickness is zero. The tools effect (Sklar and Dietrich, 2001) is ignored. Bedrock incision creates an equivalent amount of sediment that is added to the regolith thickness at that cell at the end of the timestep.

Regolith production

Regolith is produced using an exponential rule (such that production rate falls off exponentially with regolith thickness) throughout (e.g. Heimsath *et al.*, 1997). The e-folding lengthscale for the falloff of regolith production rate with depth can be prescribed to vary between rock types. We ignore the density difference between bedrock and regolith in this paper; it is likely significant in our study landscapes, but the effect would be equivalent to adjusting other model parameters. Because we are using abstracted transport rules and our goal is not to determine parameter values to match a particular landscape, we do not add this layer of extraneous calculation.

Regolith transport

Regolith transport velocity is calculated as the sum of two components: a 'hillslope' or diffusive component that is solely a function of local slope; and a 'fluvial' or advective component that is a function of both slope and drainage area. Both components are applied everywhere on the model space; where the advective term dominates, channels tend to form (Perron *et al.*, 2008). The transport velocity is decomposed into x- and y-oriented vectors (using the D_∞ flow directions), which are multiplied by cross-sectional area Hdx or Hdy. This yields fluxes Q_x and Q_y (in m^3/yr). The value of H is the thickness of the mobile layer, which is the lesser of the regolith thickness and a cutoff mobile thickness (here, 5 cm). The transport velocity is assumed

constant over the entire mobile thickness of regolith. The erosion or deposition rate (regolith thinning or thickening) is calculated as the divergence of regolith flux (Q_x and Q_y) at each cell. In the case of erosion, no more than the existing thickness of regolith can be removed in a timestep. If a cell is stripped of regolith during a timestep, the bedrock incision rule is applied there over the remaining fraction of the timestep.

Linear transport (in which regolith flux is directly proportional to slope) leads to hillslopes that are parabolic in profile in the direction of transport. In the Book Cliffs, the shale badlands have parabolic tops but straight sides at a consistent slope of 30° to 35°, reflecting a shallow (typically, a few centimeters) landsliding process that efficiently removes regolith from slopes of this steepness. This process could be represented by a non-linear-with-slope regolith transport relation (e.g. Roering *et al.*, 2001); however, we use linear hillslope transport throughout because it allows for much larger timesteps and a faster exploration of the other model parameters. Roering *et al.* (2001) describe in detail how a landscape's predicted relief and response time to external forcing differ between linear and non-linear transport rules.

Suspended sediment

We know of no well-tested transport relations for suspended sediment that apply to first-order ephemeral channels with the extreme slopes of the landscape we are modeling. Nonetheless, in the case of the Book Cliffs, most of the regolith that enters channels is suspended during occasional flow events and removed entirely from the system, because it is fine-grained sand or silt. Redeposition does occur on any low slopes within the channel profile, as evidenced by mud puddles and micro-fans observable in the field. To approximate these effects in a manner consistent with our other transport relations, we again use stream power to calculate a fraction of the mobile thickness removed in suspension. We define a reference stream power, above which the entire mobile thickness of regolith is removed in suspension, and below which the fraction of this thickness removed scales linearly with stream power.

This rule smoothly tapers the erosion in upper reaches of a channel between fully transport-limited and fully detachment-limited conditions. Importantly, this inhibits the formation of unrealistically large, abrupt channel heads (which can only be represented at the size of the grid spacing). For our purposes, we set the reference stream power for suspension fairly low, so that channels become detachment-limited over most of their length, as is the case in the landscapes we seek to model.

Rockfall

Because the model tracks dz/dt, we need a way to approximate backwearing in horizontal directions by rockfall from a steep cliff. We detect viable rockfall source pixels by a slope-threshold and rocktype criterion, and 'fail' these pixels one by one at random until either the maximum rockfall volume specified for a particular timestep is satisfied or until no more sources meet the failure criterion. This allows the rockfall rate to adjust to topographic changes dynamically, while allowing us to prescribe a maximum rate that can be changed between experiments to mimic a setting wherein cliff retreat is limited by the rate of rockfall. The slope threshold can vary from rocktype to rocktype, and we can turn off rockfall entirely on some rocktypes by setting the slope threshold to infinity. This gives us better experimental control on where rockfall debris is sourced and keeps us from having to track multiple debris types, which would add significant complexity to the model.

When a pixel 'fails' it is reduced in elevation to that of its highest downhill neighbor. This results in deeper failures where slopes are uniformly steep, and shallower ones where slope angles are mixed. Because the failure depth is determined independently of the prescribed rockfall rate, excess material delivered in one timestep is counted against the quota for the next timestep.

Because the model cellsize is always larger than most rockfall events in our field settings, and material can only be removed in the (x,y) directions in single-pixel increments, each pixel failure represents an amalgam of many 'real-life' rockfall events. This renders the process cellsize-dependent, because with larger pixels, fewer can fail at a given timestep before the erosion quota is met. The overall amount of debris delivered per time is the same, however; the cellsize dependence is only in the distribution of event sizes. We mitigate this effect by performing our experiments at a standard grid spacing of 10 m throughout, within the range of typical large rockfall events on the Book Cliffs.

Cells downhill of the source pixel and within 30° azimuth of its topographic aspect are weighted according to their topographic properties. Each cell's 'weight' determines how much of the rockfall debris from each event is placed there. The relative amount of rockfall debris that a particular cell receives is (1) a declining exponential function of distance from the source pixel, with an e-folding distance of 100–300 m; (2) an inverse function of slope angle, such that the probability of deposition scales as 1/slope; (3) a curvature dependence that prevents material from being deposited on 'flat' slopes at the crest of very thin ridges and enhances the probability of deposition in depressions.

Having calculated a volume of rockfall $dx \times dy \times H_f$, where H_f is the failure height, rockfall debris is spread across the landscape according to the normalized weighting of the downhill cells. The thickness of the resulting debris layer after all events have completed in a timestep is tracked, and is added to the topography; erosion in a given timestep is subtracted from this layer until it reaches zero thickness. New rockfall debris is incorporated into the regolith layer if it is thinner than the regolith; otherwise, the existing regolith is incorporated into the rockfall debris layer. The debris erodibility parameters are assigned to the property grids in binary fashion: where there is debris, the properties of the debris are assigned.

This algorithm for rockfall distribution is computationally efficient (compared to distributing the debris by calculating its travel downhill in a more physical way), and it is flexible, in that the distribution weighting functions can be modified as needed for different landscapes, or as informed by physical descriptions of rockfall distribution. In practice, the rules described earlier result in qualitatively-realistic distributions of debris, with most of the deposition in channels and at low slopes near the rockfall source. In this paper, we use the same deposition rules for all model runs.

Stratigraphy

An arbitrary number of different stratigraphic units can be inserted in the model. Stratigraphic units are defined as rectangular prisms. Non-rectilinear layers and dipping stratigraphy can be constructed from many overlapping rectilinear layers (whose minimum dimension in the x,y plane is one grid cell, and whose vertical dimension can be arbitrary). For these experiments, we use a single, horizontal layer of hard caprock ('sandstone') of 50 m thickness above more erodible rock ('shale'). Erodibility is defined by the coefficients of the stream-power rule and the rate at which the rock weathers to produce regolith; these are defined independently as a list of 'rock types' and each stratigraphic unit is assigned the desired rock type from this list. Where the topographic surface (upon which erosion calculations are performed) intersects a stratigraphic

unit, each property grid representing an erosion rule coefficient is set to the properties of the corresponding rock type. In the caprock, both the regolith production rate and the stream-power coefficient are set very low (three or more orders of magnitude lower than those of the underlying shale) in order to limit fluvial erosion at the low slopes of the upper surface and promote formation of very steep slopes at the clifftop.

Initial condition

We use a standard initial condition based on a synthetic landscape generated externally to the model. In this way, the initial condition for all runs is identical down to the random noise. Random noise is generated at the cellular scale then progressively filtered over wider and wider windows, so that random topographic perturbations occur at every horizontal scale between 20 cells (here, 200 m) and one cell (10 m). We find that this treatment reduces the spurious occurrence of linear, grid-parallel channels that commonly arise in regular-grid LEMs.

The initial landscape (Figure 10A) consists of an upper plane representing the clifftop that tilts toward the back of the model ('North'; $+y$ direction) with a very small slope value of 0·001. At $y = 1000$ m, the elevation of this plane is 500 m, representing the top of a 500 m cliffband. From this line, the landscape dips down in the $-y$ direction toward the front of the model at 32°; this means that the base level of the landscape is zero meters over the first 200 m in the y direction, giving rockfall debris an outlet in the initial stages. The initial cliff slope angle of 32° allows for faster spin-up times than starting with a steeper cut, as any streams that form are closer to their preferred grade initially, and rockfall rates are not artificially enhanced by the steepness of the landscape; in fact, because the initial cut is less steep than the threshold for rockfall, rockfall rates are zero until the upper reaches of the streams steepen to the threshold slope angle. The slight back-tilt applied to the upper plane has an important function: it naturally sets the drainage divide at the top of the cliffband and maintains it there throughout the model run. In this way we control for effects of changing drainage area. Because there is no discharge from beyond the top of the cliff entering the cliffband channels, drainage area does not change as the cliff retreats. This feature was inspired by the section of the Book Cliffs that we describe earlier.

Boundary conditions

The $y = 0$ and $y = y_{max}$ boundary conditions are held at a constant elevation, zero regolith thickness, and zero slope for a border width of five cells throughout each run. The $x = 0$ and $x = x_{max}$ boundaries are periodic.

References

Berlin MM. 2009. *Knickpoint Migration and Landscape Evolution on the Roan Plateau, Western Colorado*, PhD Thesis. University of Colorado, Boulder, CO; 242 pp.

Berlin MM, Anderson RS. 2007. Modeling of knickpoint retreat on the Roan Plateau, western Colorado. *Journal of Geophysical Research* **112**: F03S06. DOI. 10.1029/2006JF000553

Berlin MM, Anderson RS. 2009. Steepened channels upstream of knickpoints: Controls on relict landscape response. *Journal Geophysical Research* **114**: F03018. DOI. 10.1029/2008JF001148

Bureau of Land Management (BLM). 2004. *Roan Plateau Planning Area Resource Management Plan Amendment and Environmental Impact Statement*, Draft: November 2003. US Department of the Interior: Washington, DC; 618 pp.

Burnett BN, Meyer GA, McFadden LD. 2008. Aspect-related microclimatic influences on slope form and processes, northeastern Arizona. *Journal of Geophysical Research* **113**: F03002. DOI. 10.1029/2007JF000789

Butler DL. 1985. *Discharge and Water Quality of Springs in Roan and Parachute Creek Basins, Northwestern Colorado, 1981–1983*, Water Resources Investigation Report 85-4078. US Geological Survey: Lakewood, CO.

Crosby BT, Whipple KX. 2006. Knickpoint initiation and distribution within fluvial networks: 236 waterfalls in the Waipaoa River, North Island, New Zealand. *Geomorphology* **82**: 16–38.

Culling WEH. 1960. Analytical theory of erosion. *The Journal of Geology* **68**(3): 336–344.

Densmore AL, Ellis MA, Anderson RS. 1998. Landsliding and the evolution of normal-fault-bounded mountains. *Journal of Geophysical Research* **103**(B7): 15,203–215,219.

Dietrich WE, Bellugi DG, Sklar LS, Stock JD, Heimsath AM, Roering JJ. 2003. Geomorphic transport laws for predicting landscape form and dynamics. *Geophysical Monograph* **135**: 103–132.

Gilbert GK. 1877. Report on the geology of the Henry Mountains [Utah]. *Publication of the Powell Survey*. US Geological Survey: Reston, VA; 160.

Hail WJ Jr. 1992. *Geology of the Central Roan Plateau Area, Northwestern Colorado*, US Geological Survey Bulletin 1787-R. US Geological Survey: Reston, VA; 1–26.

Heimsath AM, Dietrich WE, Nishiizumi K, Finkel RC. 1997. The soil production function and landscape equilibrium. *Nature (London)* **388**(6640): 358–361.

Howard AD. 1988. Groundwater sapping experiments and modeling. In *Sapping Features of the Colorado Plateau, a Comparative Planetary Geology Field Guide*, Howard AD, Kochel RC, Holt HE (eds). National Aeronautics and Space Administration Special Publication 491. National Aeronautics and Space Administration: Washington, DC; 71–83.

Howard AD. 1994. A detachment-limited model of drainage basin evolution. *Water Resources Research* **30**(7): 2261–2285.

Howard AD. 1995. Simulation modeling and statistical classification of escarpment planforms. *Geomorphology* **12**: 187–214.

Howard AD. 1997. Badland morphology and evolution: Interpretation using a simulation model. *Earth Surface Processes and Landforms* **22**: 211–227.

Howard AD, Kerby G. 1983. Channel changes in badlands. *Geological Society of America Bulletin* **94**: 739–752.

Howard AD, Selby MJ. 1994. Rock slopes. In *Geomorphology of Desert Environments*, Abrahams AD, Parsons AJ (eds). Chapman and Hall: London; 123–172.

King LC. 1953. Canons of landscape evolution. *GSA Bulletin* **64**: 721–752.

Kirby E, Whipple K. 2001. Quantifying differential rock-uplift rates via stream profile analysis. *Geology* **29**: 415–418.

Koons ED. 1955. Cliff retreat in the southwestern United States. *American Journal of Science* **253**(1): 44–52.

Lamb MP, Dietrich WE. 2009. The persistence of waterfalls in fractured rock. *GSA Bulletin* **121**(7–8): 1123–1134. DOI. 10.1130/B26842.1

Luo W, Arvidson RE, Sultan M, Becker R, Crombie MK, Sturchio N, El Alfy Z. 1997. Ground-water sapping processes, Western Desert, Egypt. *GSA Bulletin* **109**(1): 43–62.

Moore JR, Sanders JW, Dietrich WE, Glaser SD. 2009. Influence of rock mass strength on the erosion rate of alpine cliffs. *Earth Surface Processes and Landforms* **34**(10): 1339–1352. DOI. 10.1002/esp.1821

Oberlander TM. 1977. Origin of segmented cliffs in massive sandstones of southeastern Utah. In *Geomorphology in Arid Regions. A Proceedings Volume of the Annual Geomorphology Symposia Series*, Doehring D (ed.). Citizen Printing Co., Fort Collins, CO; 79–114.

Olson RW. 1974. *Valley Morphology and Landslides, Roan Creek and Parachute Creek Basins, Western Colorado*, Masters Thesis. Colorado State University, Fort Collins, CO; 88 pp.

Perez FL. 1989. Talus fabric and particle morphology on Lassen Peak, California. *Geografiska Annaler* **71A**(1–2): 43–57.

Perron JT, Dietrich WE, Kirchner JW. 2008. Controls on the spacing of first-order valleys. *Journal of Geophysical Research* **113**: F04016. DOI. 10.1029/2007JF000977

Repka JL, Anderson RS, Finkel RC. 1997. Cosmogenic dating of fluvial terraces, Fremont River, Utah. *Earth and Planetary Science Letters* **152**(1–4): 59–73.

Roering JJ, Kirchner JW, Dietrich WE. 2001. Hillslope evolution by nonlinear, slope-dependent transport; steady state morphology and equilibrium adjustment timescales. *Journal of Geophysical Research* **106**(B8): 16,499–416,513.

Roering JJ, Perron JT, Kirchner JW. 2007. Functional relationships between denudation and hillslope form and relief. *Earth and Planetary Science Letters* **264**: 245–258.

Schmidt K-H. 2009. Hillslopes as evidence of climatic change. In *Geomorphology of Desert Environments*, Parsons AJ, Abrahams AD (eds), 2nd edition. Springer: Berlin; 675–694. DOI. 10.1007/978-1-4020-5719-9-22

Selby MJ. 1982. *Hillslope Materials and Processes*. Oxford University Press: New York; 264 pp.

Sklar LS, Dietrich WE. 2001. Sediment and rock strength controls on river incision into bedrock. *Geology (Boulder)* **29**(12): 1087–1090.

Snyder NP, Whipple KX, Tucker GE, Merritts D. 2000. Landscape response to tectonic forcing: DEM analysis of stream profiles in the Mendocino Triple Junction region, northern California. *Geological Society of America Bulletin* **112**(8): 1250–1263.

Tarboton DG. 1997. A new method for the determination of flow directions and contributing areas in grid digital elevation models. *Water Resources Research* **33**(2): 309–319.

Taylor OJ. 1987. Hydrologic system of Piceance Basin. In *Oil Shale, Water Resources, and Valuable Minerals of the Piceance Basin, Colorado: The Challenge and Choices of Development*, Taylor OJ (ed.), US Geological Survey Professional Paper 1310. US Geological Survey, Reston, VA; 63–76.

Tucker GE, Slingerland R. 1997. Drainage basin responses to climate change. *Water Resources Research* **33**(8): 2031–2047.

Tucker G, Lancaster S, Gasparini N, Bras R. 2001. *The Channel-hillslope Integrated Landscape Development Model (CHILD), Landscape Erosion and Evolution Modeling*. Kluwer Academic/Plenum Publishers: New York.

Weissel JK, Seidl MA. 1997. Influence of rock strength properties on escarpment retreat across passive continental margins. *Geology* **25**(7): 631–634.

Whipple KX, Tucker GE. 1999. Dynamics of the stream power river incision model: implications for height limits of mountain ranges, landscape response timescales and research needs. *Journal of Geophysical Research* **104**: 17,661–17,674.

Whipple KX, Tucker GE. 2002. Implications of sediment-flux dependent river incision models for landscape evolution. *Journal of Geophysical Research* **107**: B2. DOI. 10.1029/2000JB000044

Wobus C, Whipple KX, Kirby E, Snyder N, Johnson J, Spyropolou K, Crosby B, Sheehan D. 2006. Tectonics from topography: procedures, promise, and pitfalls. In *Tectonics, Climate, and Landscape Evolution*, Willett SD, *et al*. (eds), Geological Society of America Special Paper 398. The Geological Society of America: Boulder, CO; 55–74. DOI. 10.1130/2006.2398(04)